Plant Biotechnology Journal
Open Access

Plant Biotechnology Journal (2025) **23**, pp. 156–173 doi: 10.1111/pbi.14486

PAM-relaxed and temperature-tolerant CRISPR-Mb3Cas12a single transcript unit systems for efficient singular and multiplexed genome editing in rice, maize, and tomato

Shishi Liu[1,2,†], Yao He[1,2,†], Tingting Fan[2], Meirui Zhu[3], Caiyan Qi[2], Yanqin Ma[4], Mengqiao Yang[5], Liang Yang[4], Xu Tang[1], Jianping Zhou[2], Zhaohui Zhong[2], Xueli An[3,*], Yiping Qi[6,7,*] and Yong Zhang[1,2,*]

[1]*Integrative Science Center of Germplasm Creation in Western China (Chongqing) Science City, Chongqing Key Laboratory of Tree Germplasm Innovation and Utilization, School of Life Sciences, Southwest University, Chongqing, China*
[2]*Department of Biotechnology, School of Life Sciences and Technology, Center for Informational Biology, University of Electronic Science and Technology of China, Chengdu, China*
[3]*Research Institute of Biology and Agriculture, University of Science and Technology Beijing, Beijing, China*
[4]*Horticulture Research Institute, Sichuan Academy of Agricultural Sciences, Chengdu, Sichuan, China*
[5]*Faculty of Biology, Ludwig-Maximilians-Universität München, Planegg-Martinsried, Germany*
[6]*Department of Plant Science and Landscape Architecture, University of Maryland, College Park, Maryland, USA*
[7]*Institute for Bioscience and Biotechnology Research, University of Maryland, Rockville, Maryland, USA*

Received 14 May 2024;
revised 12 August 2024;
accepted 25 September 2024.
**Correspondence* (email zhangyong916@uestc.edu.cn (Y.Z.); email yiping@umd.edu (Y.Q.); email xuelian@ustb.edu.cn (X.A.))
†These authors contributed equally to this work.

Keywords: CRISPR-Mb3Cas12a, multiplex editing, promoter editing, rice, maize, tomato.

Summary

Class 2 Type V-A CRISPR-Cas (Cas12a) nucleases are powerful genome editing tools, particularly effective in A/T-rich genomic regions, complementing the widely used CRISPR-Cas9 in plants. To enhance the utility of Cas12a, we investigate three Cas12a orthologs—Mb3Cas12a, PrCas12a, and HkCas12a—in plants. Protospacer adjacent motif (PAM) requirements, editing efficiencies, and editing profiles are compared in rice. Among these orthologs, Mb3Cas12a exhibits high editing efficiency at target sites with a simpler, relaxed TTV PAM which is less restrictive than the canonical TTTV PAM of LbCas12a and AsCas12a. To optimize Mb3Cas12a, we develop an efficient single transcription unit (STU) system by refining the linker between Mb3Cas12a and CRISPR RNA (crRNA), nuclear localization signal (NLS), and direct repeat (DR). This optimized system enables precise genome editing in rice, particularly for fine-tuning target gene expression by editing promoter regions. Further, we introduced Arginine (R) substitutions at Aspartic acid (D) 172, Asparagine (N) 573, and Lysine (K) 579 of Mb3Cas12a, creating two temperature-tolerant variants: Mb3Cas12a-R (D172R) and Mb3Cas12a-RRR (D172R/N573R/K579R). These variants demonstrate significantly improved editing efficiency at lower temperatures (22 °C and 28 °C) in rice cells, with Mb3Cas12a-RRR showing the best performance. We extend this approach by developing efficient Mb3Cas12a-RRR STU systems in maize and tomato, achieving biallelic mutants targeting single or multiple genes in T_0 lines cultivated at 28 °C and 25 °C, respectively. This study significantly expands Cas12a's targeting capabilities in plant genome editing, providing valuable tools for future research and practical applications.

Introduction

Clustered regularly interspaced short palindromic repeats (CRISPR)/CRISPR-associated (Cas) systems, originally discovered as adaptive immune systems in bacteria and archaea, have been widely used for precise genome modification in plants. The development of CRISPR-Cas offers promising tools to tackle global agricultural challenges through introducing desirable traits into crops, such as improved yield (Liu *et al.*, 2017, 2021; Ren *et al.*, 2021a; Wu *et al.*, 2022; Yuste-Lisbona *et al.*, 2020; Zhang *et al.*, 2019; Zhou *et al.*, 2019), enhanced nutritional content (Arruabarrena *et al.*, 2023; Dong *et al.*, 2020; Li *et al.*, 2018; Sanchez-Leon *et al.*, 2018; Zhou *et al.*, 2023), increased resistance to diseases (Fu *et al.*, 2024; Liu *et al.*, 2018; Mahas *et al.*, 2019; Oliva *et al.*, 2019; Peng *et al.*, 2017; Wang *et al.*, 2014; Xu *et al.*, 2019b), and environmental stresses (Alfatih *et al.*, 2020; Huang *et al.*, 2019; Hui *et al.*, 2024; Liu *et al.*, 2020; Su *et al.*, 2023; Wang *et al.*, 2024; Zhang *et al.*, 2018; Zhou *et al.*, 2021, 2022).

Cas12a, a Class 2 Type V-A CRISPR-Cas nuclease, has emerged as a promising alternative to Cas9 in the field of genome editing. Cas12a exhibits a unique protospacer adjacent motif (PAM) recognition that is rich in A/T content (Zetsche *et al.*, 2015), in contrast to SpCas9 (Jinek *et al.*, 2012), which utilizes a G/C-rich PAM. This distinct PAM requirement enables Cas12a to effectively target genomic regions that may be inaccessible to SpCas9. Unlike Cas9, Cas12a only needs a short CRISPR RNA (crRNA) for DNA targeting. Moreover, Cas12a

possesses RNase activity for crRNA array processing, making it an excellent platform for multiplexed editing (Hui *et al.*, 2024; Malzahn *et al.*, 2019; Tang *et al.*, 2019; Tang and Zhang, 2023; Wang *et al.*, 2017; Xu *et al.*, 2019a; Zetsche *et al.*, 2017; Zhang *et al.*, 2021b). Cas12a generates staggered double-strand breaks (DSBs), which results in larger deletions, making Cas12a a preferable tool for the deletion of multiple base motifs or specific non-coding RNAs within the genome (Tang and Zhang, 2023; Zhang *et al.*, 2021b; Zhou *et al.*, 2017, 2021, 2022, 2023). Furthermore, Cas12a has demonstrated higher targeting specificity compared to Cas9 in mammalian cells and plants (Kim *et al.*, 2016; Kleinstiver *et al.*, 2016; Ren *et al.*, 2021b; Tang *et al.*, 2018). This improved specificity minimizes off-target effects and enhances the accuracy of genome editing in these organisms.

The versatility and simplicity of the CRISPR-Cas12a system enable the modification of numerous genes in elite cultivars, which may be challenging or impractical to achieve through conventional breeding methods. However, the targeting scope of most Cas12a nucleases is limited by the restrictive TTTV (V = A, C, and G) PAM. To overcome this limitation, researchers have attempted various strategies to expand the editing scope of Cas12a, including exploring novel Cas12a orthologs or engineering Cas12a nucleases with relaxed PAM requirements in vitro and mammalian cells (Gao *et al.*, 2017; Jacobsen *et al.*, 2020; Teng *et al.*, 2019; Toth *et al.*, 2018, 2020; Zetsche *et al.*, 2020). In the context of plants, certain Cas12a orthologs, such as FnCas12a (Zhong *et al.*, 2018) and Mb2Cas12a (Zhang *et al.*, 2021b), have been demonstrated to target some VTTV PAM sequences. Additionally, engineered Cas12a variants have been developed to target altered PAM sequences (Zhong *et al.*, 2018). However, compared to the abundant resources of bacterial Cas12a orthologs, the repertoire of efficient CRISPR systems currently available for plant genome editing is significantly limited. Furthermore, Cas12a-mediated editing efficiency is known to be reduced under low-temperature conditions (Bernabe-Orts *et al.*, 2019; Lee *et al.*, 2019; Malzahn *et al.*, 2019). Although this challenge can be partially addressed through protein engineering, such as the development of enAsCas12a (Kleinstiver *et al.*, 2019), ttLbCas12a (Schindele and Puchta, 2020), and LbCas12a-RRV (Zhang *et al.*, 2023), it is noteworthy that temperature-tolerant nucleases in plants have thus far been developed exclusively based on LbCas12a, which largely relies on the TTTV PAM. Moreover, to enable versatile genome engineering in plants, there is a need for a CRISPR-Cas12a system with both high efficiency and a broad targeting scope.

To search for additional Cas12a orthologs for editing relaxed VTTV PAMs, we comprehensively assess three Cas12a orthologs and identified Mb3Cas12a as a promising Cas12a nuclease. Next, we developed efficient STU systems by improving the linker, NLS, and DR sequence. Moreover, we successfully engineered temperature-tolerant variants, Mb3Cas12a-R and Mb3Cas12a-RRR, which displayed significantly increased editing efficiency at lower temperatures. By utilizing the optimizing Mb3Cas12a-STU system, we applied CRISPR-Cas12a promoter editing (CAPE) strategy to achieve efficient promoter editing of two target genes, *OsGBSS1* and *OsD18*, in rice. Furthermore, with the temperature-tolerant variant Mb3Cas12a-RRR, we successfully develop efficient STU genome editing systems for maize and tomato. By expanding our efforts to more plant species, we demonstrated the versatility and scalability of the Mb3Cas12a toolbox in achieving efficient genome editing.

Results

Comparison of Cas12a orthologs reveals robust genome editing by Mb3Cas12a at both TTTV and TTV PAM sites in rice

Many demonstrated Cas12a orthologs require the TTTV PAM, which limits their applications in plants. To broaden the scope of Cas12a genome editing, we selected three Cas12a orthologs: Mb3Cas12a, PrCas12a, and HkCas12a. These orthologs have shown high editing efficiency at VTTV PAM sites in human cells or vitro, but their potential in plant editing has not been well-established (Teng *et al.*, 2019; Zetsche *et al.*, 2020). We employ a dual RNA Polymerase II (Pol II) promoter expression system to express Cas12a/crRNA (Tang *et al.*, 2017) (Figure 1a). These three Cas12a orthologs exhibit a close evolutionary relationship to other Cas12a orthologs that have been previously studied in plants, including LbCas12a, FnCas12a, and Mb2Cas12a (Figure 1b). Therefore, we utilized these well-known Cas12a orthologs as controls to evaluate the editing efficiency of the new Cas12a orthologs.

The editing efficiencies of the Cas12a orthologs are evaluated at three TTTV PAM target sites and three VTTV PAM target sites in rice protoplasts at 32 °C, using next-generation sequencing (NGS). At the three TTTV PAM target sites, Mb3Cas12a exhibited a mutation frequency of approximately 40.0% or higher at all sites, which is comparable to LbCas12a and Mb2Cas12a. PrCas12a showed high mutant efficiency at the TTTG site (>40.0%), but lower efficiency at the TTTA and TTTC sites (3.9%~7.3%). HkCas12a showed high mutant efficiency at both the TTTC and TTTG sites (36.4%~60.8%), but lower efficiency at the TTTA sites (8.3%) (Figure 1c). Furthermore, we assess the editing efficiency at three VTTV PAM target sites. Mb3Cas12a still exhibit a robust efficiency at all sites, which is comparable to or higher than FnCas12a and Mb2Cas12a, both of which have been shown to have high efficiency at VTTV PAM sites in plants (Zhang *et al.*, 2021b; Zhong *et al.*, 2018). PrCas12a and HkCas12a conferred an efficient editing >10.0% at the TTC site, however, they displayed much lower efficiency at the TTG site and no editing activity at the TTA site (Figure 1d). The narrower dynamic range of editing efficiency across different target sites, either with TTTV PAMs (Figure 1c) or with VTTV PAMs (Figure 1d), suggests that Mb3Cas12a is a more robust Cas12a nuclease than FnCas12a and Mb2Cas12a.

To further validate the robust editing efficiency of Mb3Cas12a, as observed in rice protoplasts, we conducted assessments in stable transgenic rice lines. A total of eight target sites were investigated, consisting of three sites with TTTV PAM and five sites with VTTV PAM. The results showed that Mb3Cas12a could induce mutagenesis at all targeted sites, with editing efficiencies ranging from 70.0% to 100% at TTTV PAM sites and 20.0% to 70.0% at VTTV PAM sites (Figure 1e). Furthermore, the biallelic editing was observed at all eight target sites, with average efficiency of ~72.0% at TTTV PAM sites and ~20.0% at VTTV PAM sites (Figure 1e and Figure S1). Mutation in the *OsGW2* gene leads to changes in rice grain morphology (Song *et al.*, 2007). We examined three different *osgw2* mutants and, as expected, they all showed significant increase in grain width and grain thickness (Figure 1f).

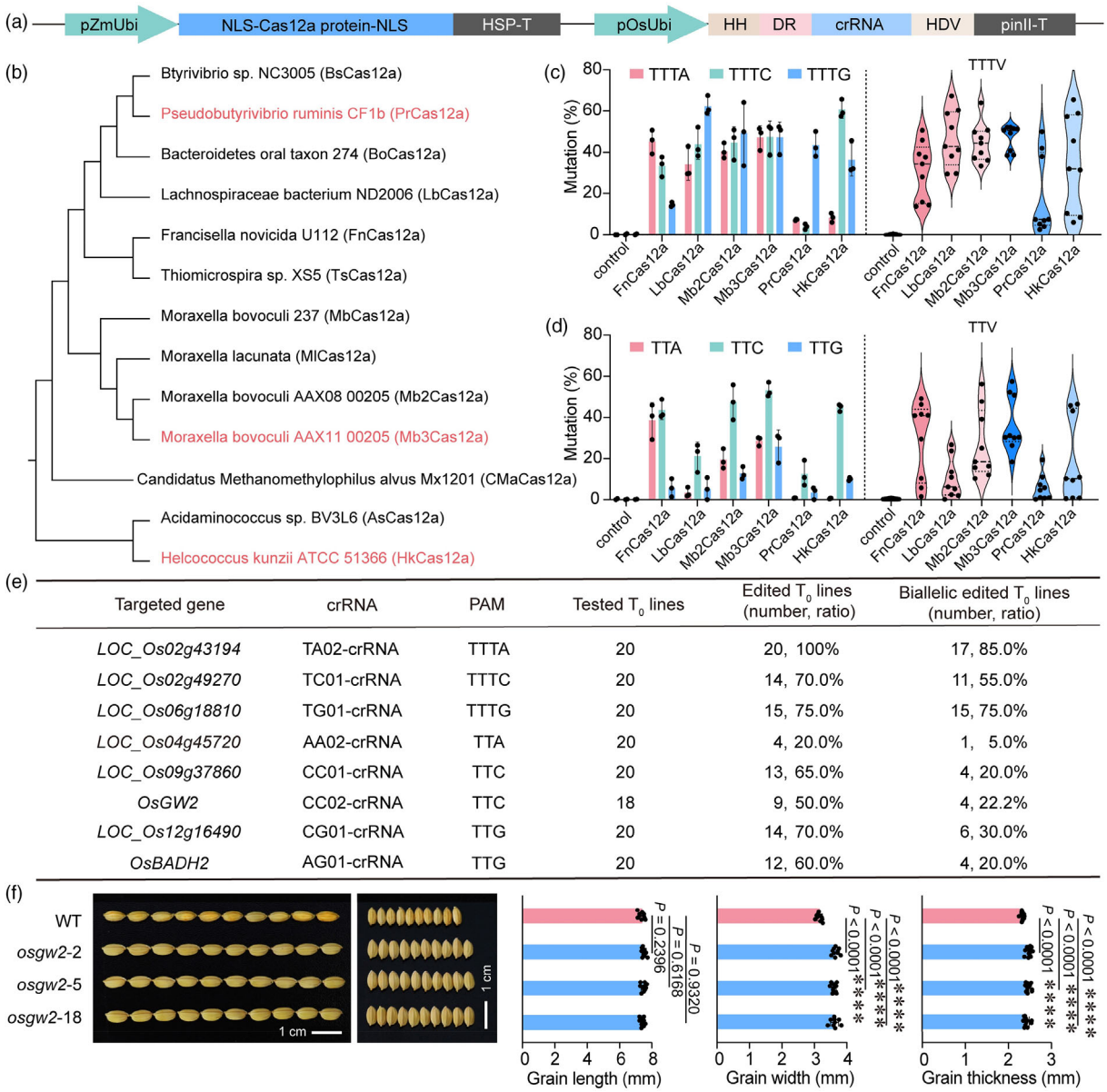

Targeted gene	crRNA	PAM	Tested T_0 lines	Edited T_0 lines (number, ratio)	Biallelic edited T_0 lines (number, ratio)
LOC_Os02g43194	TA02-crRNA	TTTA	20	20, 100%	17, 85.0%
LOC_Os02g49270	TC01-crRNA	TTTC	20	14, 70.0%	11, 55.0%
LOC_Os06g18810	TG01-crRNA	TTTG	20	15, 75.0%	15, 75.0%
LOC_Os04g45720	AA02-crRNA	TTA	20	4, 20.0%	1, 5.0%
LOC_Os09g37860	CC01-crRNA	TTC	20	13, 65.0%	4, 20.0%
OsGW2	CC02-crRNA	TTC	18	9, 50.0%	4, 22.2%
LOC_Os12g16490	CG01-crRNA	TTG	20	14, 70.0%	6, 30.0%
OsBADH2	AG01-crRNA	TTG	20	12, 60.0%	4, 20.0%

Figure 1 Mb3Cas12a confers robust genome editing at both TTTV and TTV PAM sites in rice. (a) Schematic of the dual RNA polymerase II promoter system for Cas12a and crRNA expression. DR, direct repeat; HDV, hepatitis delta virus ribozyme; HH, hammerhead ribozyme; HSP-T, heat shock protein terminator; NLS, nuclear localization signal; pinII-T, proteinase inhibitor II terminator; pOsUbi, rice ubiquitin promoter; pZmUbi, maize ubiquitin promoter. (b) A phylogenetic tree of 13 Cas12a orthologs based on protein sequence alignment. (c) Genome editing efficiencies of six Cas12a orthologs at three TTTV PAM sites in rice protoplasts at 32 °C. (d) Genome editing efficiencies of six Cas12a orthologs at three TTV PAM sites in rice protoplasts at 32 °C. Control, protoplasts transformed with backbone. Three biological replicates were used. (e) Summary of editing and biallelic editing efficiencies of Mb3Cas12a on three TTTV PAM sites and five TTV PAM sites in transgenic rice T_0 lines. (f) Seed length, width, and thickness of three *osgw2* mutants and controls. Scale bars, 1 cm. For experiments in rice grain analysis, eight to ten replicates were used. The error bars denote standard deviations. Asterisks were used to denote statistical significance by Student's *t*-test (****$P < 0.0001$).

We also investigated the editing profiles of the new Cas12a orthologs at two independent target sites in rice protoplasts. The mutations induced by these Cas12a orthologs were primarily deletions (Del) (Figure 2a and Figure S2a), resulting in deletion ranging from 6 to 12 bp at the target site (Figure 2b–d and Figure S2b–d). The deletion positions span from 13 to 27 nt (Figure 2e–g). Next, we assessed the editing specificity with mismatched crRNAs and crRNAs of different length. When protospacers with mismatches were used, all three Cas12a orthologs show tolerance only for mismatches located in the last three base pairs distal from the PAM, indicating a high level of targeting specificity (Figure 2h–k). Protospacers ranging from 19 to 23 nt can generate high editing frequencies for HkCas12a and Mb3Cas12a, while PrCas12a requires longer protospacers to achieve robust activity (Figure 2l–o and Figure S2e–h). Taken together, Mb3Cas12a is an efficient and precise genome editing

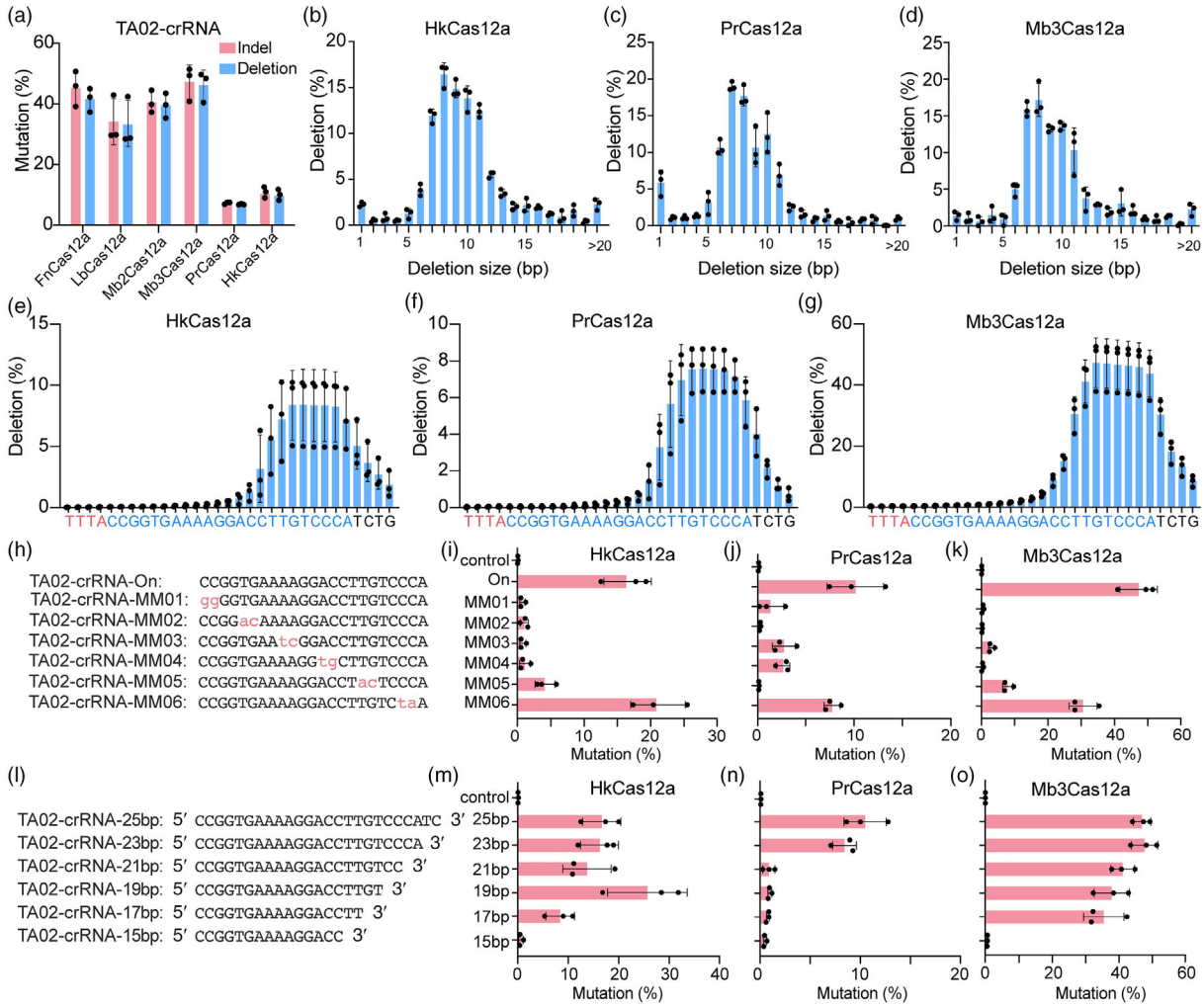

Figure 2 Analyses of genome editing profiles and specificity of Cas12a orthologs in rice protoplasts. (a) Assessment of deletion frequencies by six Cas12a orthologs. Indel, insertion and deletion. (b–d) Deletion size profile of Cas12a orthologs at the TA02-crRNA site in rice protoplasts at 32 °C. (b) (HkCas12a), (c) (PrCas12a), (d) (Mb3Cas12a). (e–g) Deletion position of Cas12a orthologs at the TA02-crRNA site in rice. (e) (HkCas12a), (f) (PrCas12a), (g) (Mb3Cas12a). (h–k) Targeting specificity of Cas12a orthologs measured with mismatched crRNAs (MM01~MM06) at the TA02-crRNA site in rice protoplasts at 32 °C. Mismatched nucleotides in crRNAs were highlighted with red in h. (i) (HkCas12a), (j) (PrCas12a), (k) (Mb3Cas12a). (l–o) Assessment of protospacer length requirements at the TA02-crRNA site in rice protoplasts at 32 °C. (m) (HkCas12a), (n) (PrCas12a), (o) (Mb3Cas12a). Three biological replicates were used. The error bars denote standard deviations.

tool in rice. Notably, with a NTTV PAM requirement, Mb3Cas12a can cover 11.5% of rice genome which is higher than that of SpCas9 with an NGG PAM requirement (10.5%) and LbCas12a with a TTTV PAM requirement (<5.0%) (Zhang *et al.*, 2021b; Zhong *et al.*, 2019).

Mb3Cas12a confers efficient multiplexed editing in rice

Previously, we showed that both single transcript unit (STU) based on a single Pol II promoter and a dual Pol II promoter system could be used to express Cas12a and crRNAs (Tang *et al.*, 2017, 2019; Zhang *et al.*, 2021b). To enable efficient multiplexed editing by Mb3Cas12a, we compared these two strategies side by side, with the crRNAs being processed by the hammerhead (HH) and hepatitis delta virus (HDV) ribozymes (STU^{HDH} and Dual Pol II) as this ribozyme processing strategy is very efficient in plants (Zhang *et al.*, 2021b) (Figure 3a). For the STU system, we also included self-processing of a crRNA array (STU^{DD}) (Figure S3a), as it is a popular strategy for expressing and processing multiple crRNAs in human cells (Zetsche *et al.*, 2015) and in plants (Tang *et al.*, 2019; Wang *et al.*, 2017; Zhang *et al.*, 2021b; Zhong *et al.*, 2018). These three multiplexed systems were compared at three target sites (*OsDEP1*-cR1, *OsROC5*-cR2, *OsmiR528*-cR3) in stable transgenic rice lines. We calculated editing efficiencies at each target site for all the multiplex systems, with 15–18 T_0 lines per construct. The dual ribozyme-based STU^{HDH} and Dual Pol II systems had comparable multiplex editing efficiency, resulting in 94.1% to 100% mutagenesis at all target sites (Figure 3b). The biallelic editing efficiencies of the STU^{HDH} system ranged from 41.2% to 94.1%, comparable to the Dual Pol II system (61.1% ~94.4%) (Figure 3c,d and Figure S4); Most of these lines contained co-edits of all three target genes (Figure 3b). However, the self-processing crRNA array system only generated 13.3% editing efficiency at each target sites, with all edits being monoallelic (Figure S3b). Taken together, dual ribozyme-based

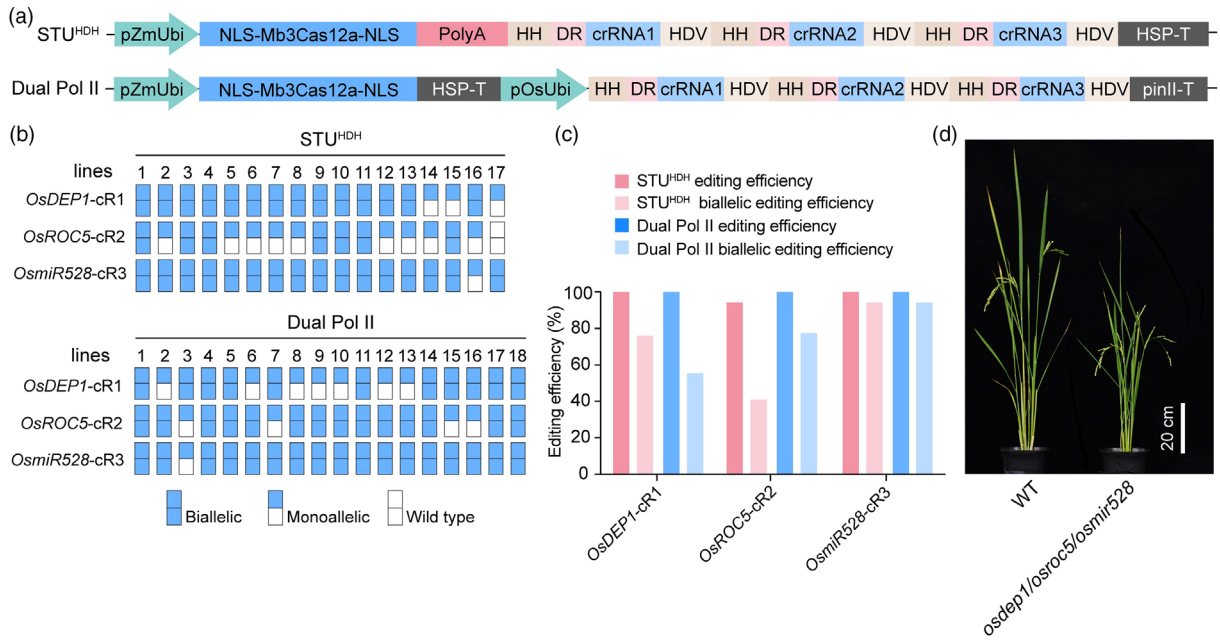

Figure 3 Optimization of CRISPR-Mb3Cas12a for plant genome editing. (a) Schematics of the single transcript unit (STU^{HDH}) and dual RNA polymerase II promoter-based (Dual Pol II) systems for CRISPR-Mb3Cas12a-mediated multiplexed editing of three target sites in rice. DR, Mb3Cas12a direct repeat; crRNA1 targets *OsDEP1*; crRNA2 targets *OsROC5*; crRNA3 targets *OsmiR528*; HDV, hepatitis delta virus ribozyme; HH, hammerhead ribozyme; HSP-T, heat shock protein terminator; NLS, nuclear localization signal; pinII-T, proteinase inhibitor II terminator; pOsUbi, rice ubiquitin promoter; pZmUbi, maize ubiquitin promoter. (b) Comparison of two multiplexed Mb3Cas12a editing systems in stable transgenic rice lines, targeting *OsDEP1*, *OsROC5*, and *OsmiR528* with three corresponding crRNAs. Seventeen to eighteen independent T_0 lines were genotyped at each target site for wild type (denoted as an empty rectangle), monoallelic mutant (denoted as a half-filled rectangle) and biallelic mutant (denoted as a fully filled rectangle). (c) Comparison of editing efficiency and biallelic editing efficiency of two multiplexed editing systems in stable transgenic rice lines with three target sites. (d) Images of *osdep1/osroc5/osmir528* triple mutant and wide type (WT) phenotypes. Scale bars, 20 cm.

STU^{HDH} system and the Dual Pol II system both conferred comparable, efficient multiplexed editing by Mb3Cas12a in rice stable plants.

Improving Mb3Cas12a STU^{HDH} systems with optimized linker, nuclear localization signal, and crRNA scaffold

Considering the dual ribozyme-based Mb3Cas12a STU^{HDH} system showed simple, compact configuration and comparable gene editing efficiency to the Dual Pol II system, we decided to focus on this STU^{HDH} system for further improvement. Firstly, we optimized the linker between Mb3Cas12a and crRNA. The Triplex (Campa *et al.*, 2019; Wilusz *et al.*, 2012) and Comp.14 (Wilusz *et al.*, 2012) were previously found to increase mRNA stability and enhance gene transcription, respectively. These two linkers, along with PolyA in the initial STU^{HDH} version, were compared at four target sites in rice protoplasts at 32 °C (Figure 4a). According to analysis the editing efficiency based on the NGS data, we found that PolyA stand out among the three systems (efficiency range from 23.7% to 42.2%). Comp.14 showed slightly lower editing efficiency than PolyA (efficiency range from 12.1% to 38.3%), while Triplex showed significantly reduced editing efficiency compared to PolyA (efficiency range from 14.7% to 27.1%) (Figure 4b).

Nuclear localization signal (NLS), due to its control of Cas nuclease's nuclear entry, is also an important element that can affect the editing efficiency. 2C NLS (nucleoplasmin NLS and SV40 NLS on the C-terminal of Cas12a) and 3C NLS (3x SV40 NLS on the C-terminal of Cas9) were previously shown to improve the editing efficiency of Cas12a (Liu *et al.*, 2019) and Cas9 (Li *et al.*, 2020; Zhong *et al.*, 2023), respectively. To optimize our STU^{HDH} system, we compared these two NLS structures, along with the default NC NLS (SV40 NLS on the N-terminal of Cas12a and nucleoplasmin NLS on the C-terminal of Cas12a) used in our original configuration (Figure 4c). We tested the three STU^{HDH} systems based on different NLS configurations at four target sites in rice protoplasts at 32 °C. We found that NC NLS was outstanding among the three systems based on analysis of the NGS data (efficiency range from 36.2% to 69.1%). 3C NLS had slightly lower editing efficiency than NC NLS (efficiency range from 32.5% to 60.5%), while 2C NLS showed overall lower editing efficiency (efficiency range from 8.5% to 65.2%) (Figure 4d).

The DR structure is an important element of CRISPR-Cas12a. Previous study found that the loop sequence of DR is a key factor affecting the editing activity of Cas12a (Teng *et al.*, 2019). We selected six DRs (4n61, 4n91, 4n96, 4n128, 4n137, and 4n149) with different loop sequences that demonstrated varying efficiencies in previous *in vitro* assays (Teng *et al.*, 2019) to observe their performance in plants. The loop sequence for the 4n61 DR is 'UUGU', for 4n91 DR it is 'UGUG', for 4n96 DR it is 'UAUG', for 4n128 DR it is 'GCAA', for 4n137 DR it is 'UUCG', and for 4n149 DR it is 'UCCU' (Figure 4e). These six DRs along with Mb3 DR were paired with Mb3Cas12a and compared at six sites in rice protoplasts at 32 °C. We found that 4n96 DR is most efficient among all 7 DRs (efficiency range from 17.3% to 59.3%). The 4n61 DR and 4n91 DR showed comparable activities to Mb3 DR, with the editing efficiency ranging from 9.6% to 46.2%, and 10.9% to 42.9%, respectively. The 4n128, 4n137,

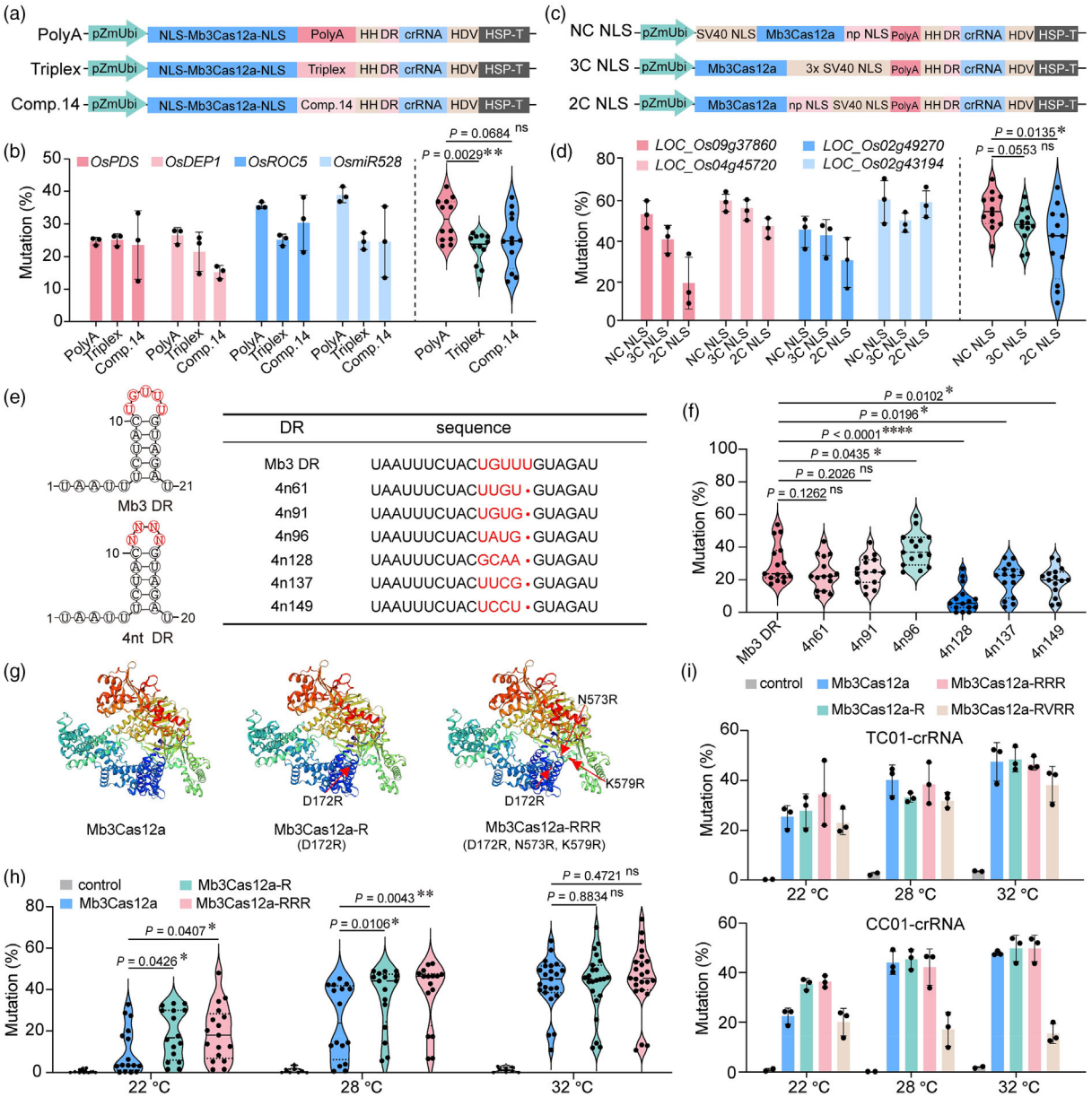

Figure 4 Optimization of CRISPR-Mb3Cas12a STU^{HDH} system for plant genome editing. (a) Schematics of three Mb3Cas12a single transcript unit (STU^{HDH}) editing systems for genome editing with different linker sequences. (b) Comparison of three Mb3Cas12a STU^{HDH} editing systems with different linkers on editing *OsPDS*, *OsDEP1*, *OsROC5* and *OsmiR528* in rice protoplasts at 32 °C. (c) Schematics of three Mb3Cas12a STU^{HDH} editing systems with different nuclear localization signal (NLS) configurations. NC NLS, SV40 NLS on the N-terminal of Cas12a and nucleoplasmin NLS (np NLS) on the C-terminal of Cas12a; 3C NLS, 3× SV40 NLS on the C-terminal of Cas12a; 2C NLS, nucleoplasmin NLS and SV40 NLS on the C-terminal of Cas12a. (d) Comparison of three Mb3Cas12a STU^{HDH} editing systems with different NLS configurations on editing *LOC_Os09g37860*, *LOC_Os04g5720*, *LOC_Os02g49270* and *LOC_Os02g43194* in rice protoplasts at 32 °C. (e) Schematics of Mb3Cas12a direct repeat (DR) and 4 nt DR (left), and sequences of seven different DRs (right). Loop sequences were colour-coded with red. (f) Comparison of seven Mb3Cas12a STU^{HDH} editing systems with different DRs at six target sites in rice protoplasts at 32 °C. (g) Predicted protein structures of Mb3Cas12a, Mb3Cas12a-R (D172R) and Mb3Cas12a-RRR (D172R/N573R/K579R) by SWISS-MODEL. (h) Comparison of Mb3Cas12a and two variants for genome editing at 22 °C, 28 °C, 32 °C on eight target sites in rice protoplasts. (i) Comparison of Mb3Cas12a and three variants for genome editing at 22 °C, 28 °C, 32 °C on two target sites with different PAM requirements in rice protoplasts. For experiments in rice protoplasts of h and i, two to three biological replicates were used. Three biological replicates were used. The error bars denote standard deviations. Asterisks were used to denote statistical significance by Student's *t*-test (*P < 0.05; **P < 0.01; ****P < 0.0001; ns, not significant).

and 4n149 DRs conferred editing activity of Mb3Cas12a (Figure 4f). We wondered that whether 4n96 DR could improve genome editing by other Cas12a orthologs. Thus, we used FnCas12a and HkCas12a to test this DR structure at four target sites in rice protoplasts. The results showed that 4n96 DR helped increase FnCas12a editing activity slightly at all sites, while this improvement was less pronounced with HkCas12a: only one site showed improved genome editing (Figure S5). Taken together,

we developed an optimized Mb3Cas12a STU^{HDH} system by using PolyA, NC NLS, and 4n96 DR.

Further optimization of the Mb3Cas12a system by protein engineering

Cas12a nucleases are sensitive to low temperatures (Malzahn *et al*., 2019). Recently, temperature-tolerant variants of AsCas12a (enAsCas12a) (Kleinstiver *et al*., 2019) and LbCas12a (ttLbCas12a) (Schindele and Puchta, 2020) were developed, showing increased genome editing activity at lower temperatures compared to their wild-type Cas12a nucleases in human cells and *Arabidopsis*. We hypothesized that installation of similar mutations to Mb3Cas12a may improve its genome editing efficiency at lower temperatures. We performed protein sequence alignment using Mega 11 and identified three conserved amino acids (D172, N573, and K579) corresponding to enAsCas12a and ttLbCas12a in Mb3Cas12a. Two Mb3Cas12a variants were engineered, Mb3Cas12a-R (D172R) and Mb3Cas12a-RRR (D172R/N573R/K579R), and subsequently tested using our optimized STU^{HDH} system (Figure 4g and Figure S6a,b).

First, we compared the editing efficiency at eight target sites in rice protoplasts, at three different temperatures (22 °C, 28 °C, and 32 °C). At 32 °C, Mb3Cas12a, Mb3Cas12a-R, and Mb3Cas12a-RRR showed comparable editing efficiency (with average efficiencies being 42.7%, 43.0%, and 45.4%, respectively) (Figure 4h). At 28 °C, Mb3Cas12a showed reduced editing efficiency; However, Mb3Cas12a-R and Mb3Cas12a-RRR maintained high editing efficiency at the level observed at 32 °C (Figure 4h). At 22 °C, genome editing efficiency of all three Mb3Cas12a nucleases dropped. However, the two engineered variants (Mb3Cas12a-R and Mb3Cas12a-RRR) conferred more than 15.0% editing efficiency at most target sites, which is up to 2 folds higher than that of Mb3Cas12a (Figure 4h). Previous study found that the Mb2Cas12a-RVRR variant could efficiently target multiple PAMs, which greatly expanded the targeting scope (Zhang *et al*., 2021b). Thus, we also engineered RVRR (N573R/K579V/N583R/K635R) variant of Mb3Cas12a (Figure S6a,b). We tested Mb3Cas12a, Mb3Cas12a-R, Mb3Cas12a-RRR, Mb3Cas12a-RVRR at the TC01-crRNA and CC01-crRNA sites in rice protoplasts, again under three temperature conditions. At the TC01-crRNA site, the results showed that these four nucleases have comparable editing efficiencies at three temperatures (Figure 4i). Interestingly, Mb3Cas12a-RVRR showed low genome editing efficiency at the CC01-crRNA site across the three different temperatures. Consistent with our earlier observation, Mb3Cas12a-R and Mb3Cas12a-RRR showed significantly higher editing activity at the CC01-crRNA site at 22 °C (Figure 4i). We also investigated the editing profiles of these Mb3Cas12a variants at CC01-crRNA site. Not surprisingly, they showed similar editing characteristics of Mb3Cas12a, with targeted mutations being predominately multiple base deletions (Figure S6c,d). Taken together, our results demonstrated that Mb3Cas12a-R and Mb3Cas12a-RRR variants provide strong temperature-tolerance genome editing in rice.

Application of the optimized CRISPR-Mb3Cas12a system for promoter editing

Promoter editing represents an innovative approach to introduce quantitative trait variation (QTV) in crops (Liu *et al*., 2021; Rodriguez-Leal *et al*., 2017; Tang and Zhang, 2023). Recently, we showed that Cas12a is potentially more advantageous to Cas9 for promoter editing (Zhou *et al*., 2023). In our CRISPR-Cas12a promoter editing (CAPE) system, key regions (KRs) in the promoter of interest can be targeted to produce QTV continuums in plants (Zhou *et al*., 2023). Here, we set to demonstrate that the optimized Mb3Cas12a STU^{HDH} system could enable applications of CAPE in rice. As rice stable transformation was done at a high temperature (32 °C), the WT Mb3Cas12a nuclease was used.

In our first demonstration, we targeted *Granule-bound starch synthase I* (*GBSS1*, also known as *Waxy/Wx*) gene which is responsible for amylose biosynthesis in grains (Huang *et al*., 2020; Tian *et al*., 2009). To generate QTV mutants efficiently, we construct an Mb3Cas12a STU^{HDH} multiplex editing system of the *OsGBSS1* promoter. We chose to target promoter regions with both high and low aggregate scores with 12 crRNAs so that we could obtain QTV continuum mutants efficiently (Zhou *et al*., 2023) (Figure 5a,b). Analysis of 19 T0 lines revealed editing at multiple target sites, with many being large deletions (Figure S7a,b). We tested five transgene-free homozygous T_1 promoter (Pro) editing lines that carried deletions of variable sizes for further characterization (Figure 5c and Figure S8). The reduced amylose contents in promoter editing lines could be easily visualized in the rice grains, with or without iodine staining (Figure 5d). The reduction of amylose contents in these lines was quantified (Figure 5e), which translated to overall reduced starch contents (Figure 5f). The expression levels of *OsGBSS1* were analysed in the promoter editing lines, which showed decreased mRNA in these lines (Figure 5g), consistent with the level of amylose contents (Figure 5e). Further analysis of the traits of the five promoter editing lines (Pro1 to Pro5) showed that they have other comparable phenotypes to the WT plants, based on the measurement of seed characteristics (e.g., seed morphology, seed length, seed width, and 1000-grain weight) (Figure 5h–k), plant height (Figure 5l) and architecture (Figure 5m).

In our second demonstration, we targeted *OsD18* in rice. Semidwarf and anti-lodging traits are highly valuable in crops which contribute to yield increase (Eshed and Lippman, 2019; Sasaki *et al*., 2002). Previous study revealed that *osd18* mutants had severe dwarfism but without compromising the grain size (Hu *et al*., 2018). Recently, we showed that editing of the *OsD18* promoter could generate semidwarf plants without significant compromise in yield (Zhou *et al*., 2023). We constructed a multiplex editing system of *OsD18* promoter based on our optimized Mb3Cas12a STU^{HDH} system, with 12 crRNAs designed within or spanning key regions in the promoter (Figure 6a,b). Analysis of 18 T_0 lines revealed editing at multiple target sites, with many being large deletions (Figure S7a,c). We tested 4 transgene-free homozygous T_1 rice lines that carry deletions of variable sizes to analysis (Figure 6c and Figure S9). As expected, expression analysis showed a reduction of *OsD18* in these promoter editing lines (Figure 6d). These T_1 homozygous lines collectively form a semidwarf continuum average from 78.5 cm to 98.0 cm (compared to 106.0 cm for the WT plants) (Figure 6e,g). The length of main panicles (Figure 6f,g) and seed number of the main panicles (Figure 6h) were reduced for the four promoter editing lines. However, the tiller numbers were increased in all promoter editing lines (Figure 6i). As a result, we did not observe reduction of grain yield in these promoter editing lines, based on measurement of seed length (Figure 6j), 1000-grain weight (Figure 6k), and seed setting rate (Figure 6l). Taken together, we demonstrated an efficient multiplex CAPE system in rice based on the Mb3Cas12a-STU^{HDH} system.

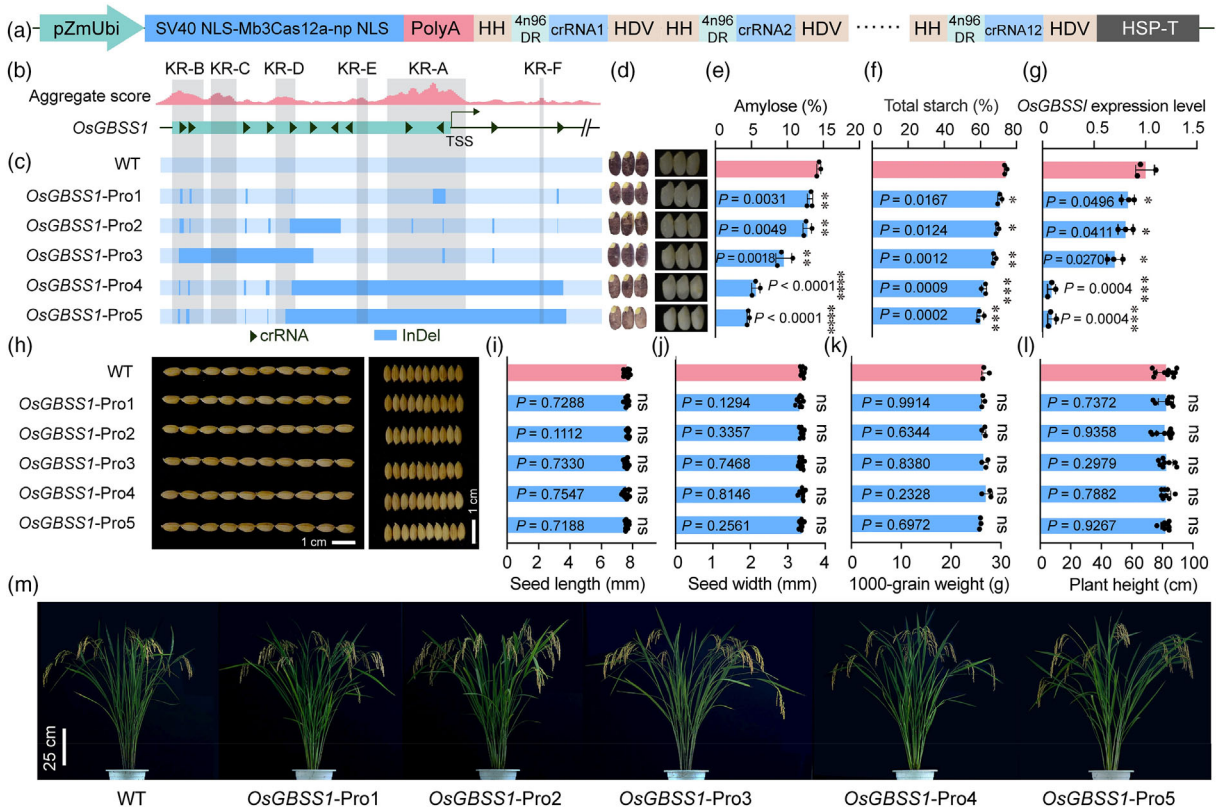

Figure 5 Application of the optimized CRISPR-Mb3Cas12a STU^{HDH} system for promoter editing of *OsGBSS1* in rice. (a) Schematic of the optimized Mb3Cas12a STU^{HDH} system for *OsGBSS1* promoter editing. 4n96 DR, 4n96 direct repeat; HDV, hepatitis delta virus ribozyme; HH, hammerhead ribozyme; HSP-T, heat shock protein terminator; np NLS, nucleoplasmin nuclear localization signal; pZmUbi, maize ubiquitin promoter. (b) Feature and aggregate scores calculated by the CAPE estimating model. The key regions (KRs) were shaded in grey (KR-A~KR-F). Each black triangle represents a crRNA, and the direction of the triangle indicates the direction of the crRNA on the promoter. TSS, transcription start site. (c) Schematic depicting the genotypes of five Mb3Cas12a-based *OsGBSS1* promoter (*OsGBSS1*-Pro) editing lines along with WT. The dark blue represents insertion and deletion (InDel). (d) Images of different *OsGBSS1* promoter editing lines following grain starch iodine staining (left) and milling (right). WT, *Nipponbare*. (e) The amylose contents of five promoter editing lines along with WT. (f) The total starch contents of five promoter editing lines along with WT. (g) The relative expression level of *OsGBSS1* of five promoter editing lines along with WT. (h–j) Seed length and width of the *OsGBSS1* promoter editing lines. (h) Seed length (right) and width (right). Scale bars, 1 cm. (i) Seed length (n = 10). (j) Seed width (n = 10). (k) Comparison 1000-grain weight of five promoter editing lines along with WT (n = 3). Statistical analysis by Student's t-test (ns, not significant). (l) Comparison plant height of five promoter editing lines along with WT (n = 8–10). Statistical analysis by Student's t-test (ns, not significant). (m) Image of different *OsGBSS1*-Pro lines along with WT. Scale bars, 25 cm. Three biological replicates were used. The error bars denote standard deviations. Asterisks were used to denote statistical significance by Student's t-test (*P < 0.05; **P < 0.01; ***P < 0.001; ****P < 0.0001; ns, not significant).

Maize microRNA editing using the Mb3Cas12a-RRR variant

Next, we wanted to demonstrate our optimized Mb3Cas12a system for genome editing in maize. With its robust performance at lower temperatures, the Mb3Cas12a-RRR variant was used (Figure 7a). We designed six target sites to test the editing efficiency in maize protoplasts. Two sites showed high editing efficiency (17.8%~28.6%) and four sites showed low editing efficiency (2.4%~4.6%) (Figure 7b), suggesting protospacer sequence and genomic location can great affect editing efficiency in maize. Next, we investigated the editing profile of Mb3Cas12a-RRR at the *ZmMIR159f*-cR site, which showed 8 bp to 11 bp deletions distal from the PAM (Figure 7c,d), similar to the editing profile observed in rice (Figure S6d). To see whether we can generate stable maize plants with targeted mutations, we conducted *Agrobacterium*-mediated maize stable transformation of Xiang 249 (X249) cultivar with the Mb3Cas12a-RRR construct targeting the *ZmMIR159f*-cR site at the *ZmMIR159f* locus (Figure 7e). We obtained four transgenic plants, and two of them were edited. One line carried biallelic editing and the other carried monoallelic editing (Figure 7f). These edits were all larger deletions (11–16 bp) (Figure 7f), consistent with the editing profile observed in protoplasts (Figure 7d). These deletions are expected to destroy microRNA mature sequence region (Figure 7f and Figure S10). Hence, Mb3Cas12a enabled efficient genetic knockout of a non-coding gene in maize.

Mb3Cas12a-RRR confers efficient multiplexed genome editing in tomato

To test the optimized Mb3Cas12a systems in dicot plants, we chose to work on tomato because it is not only a major edible vegetable but also a model crop for testing genome editing tools. Mb3Cas12a-RRR was chosen due to its robust editing activity at 22 °C. Previous studies reported that ttLbCas12a and LbCas12a-RRV could achieve high editing efficiencies in dicot plants (Schindele and Puchta, 2020; Zhang *et al.*, 2023). Thus, we decided to benchmark Mb3Cas12a-RRR with comparison to

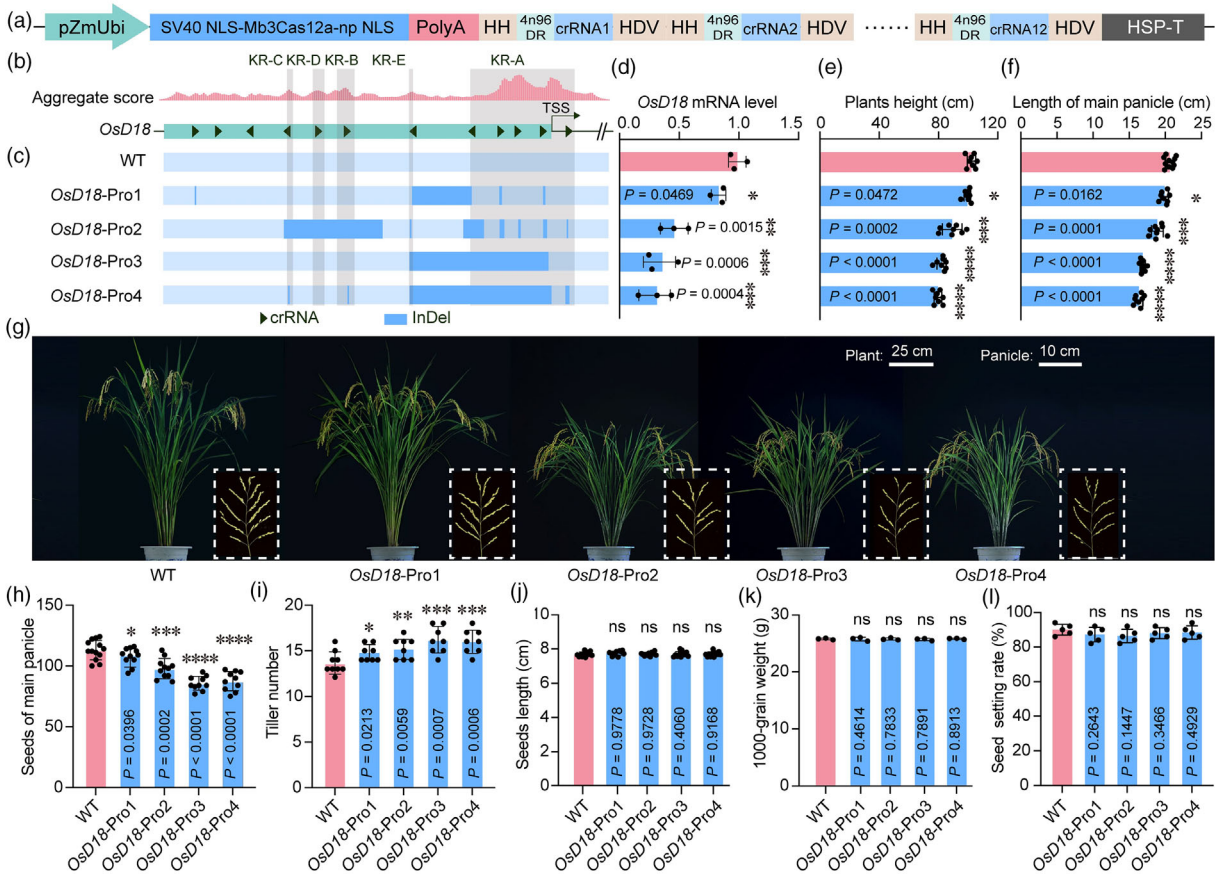

Figure 6 Application of the optimized CRISPR-Mb3Cas12a STU^{HDH} system for promoter editing of *OsD18* in rice. (a) Schematics of the optimized Mb3Cas12a STU^{HDH} system for *OsD18* promoter editing. 4n96 DR, 4n96 direct repeat; HDV, hepatitis delta virus ribozyme; HH, hammerhead ribozyme; HSP-T, heat shock protein terminator; np NLS, nucleoplasmin nuclear localization signal; pZmUbi, maize ubiquitin promoter. (b) Feature and aggregate scores calculated by the CAPE estimating model. The key regions (KRs) were shaded in grey (KR-A~KR-E). Each black triangle represents a crRNA, and the direction of the triangle indicates the direction of the crRNA on the promoter. TSS, transcription start site. (c) Schematic depicting the genotypes of five Mb3Cas12a-based *OsD18* promoter (*OsD18*-Pro) editing lines along with WT. The dark blue represents insertion and deletion (InDel). (d) The relative expression level of *OsD18* of four promoter editing lines along with WT. All data represent the mean ± s.d. of three biological replicates. (e) The plant height for four promoter editing lines along with WT (n = 8–10). (f) The length of main panicle for four promoter editing lines along with WT (n = 8–10). (g) Image of plant (left) and panicle (right; dashed-white box) phenotypes of *OsD18* promoter editing lines and control plants grown. Scale bars of plant height, 25 cm. Scale bars of panicle, 10 cm. (h–l) Field trial of *OsD18* promoter editing and control lines in a *Nipponbare* background. Grain number (h; $n \geqq 10$), tiller number (i; n = 8–10), seed length, (j; n = 8), 1000-grain weight (k; n = 3), and seed setting rate (l; n = 5) were assessed. Three biological replicates were used. The error bars denote standard deviations. Asterisks were used to denote statistical significance by Student's t-test (**P < 0.01; ns, not significant).

these two top-performing Cas12a nucleases under our optimized STU^{HDH} expression system (Figure 8a). We chose eight target sites to test these three Cas12a nucleases in tomato protoplasts. The results showed that Mb3Cas12a-RRR and LbCas12a-RRV have high editing activities in tomato, with editing efficiency >10.0% across all eight target sites (Figure 8b). The editing activities of ttLbCas12a at six sites were >10.0%, but the editing activities at two sites, *SlSGR*-cR2 and *SlCYE*-cR, were less than 10.0% (Figure 8b). Overall, Mb3Cas12a-RRR showed significantly higher editing efficiency than ttLbCas12a in tomato protoplasts. The editing profile indicated that Mb3Cas12a-RRR generated larger deletions in tomato cells (Figure 8c), consistent with the earlier data in rice and maize cells.

The high editing activity of Mb3Cas12a-RRR STU^{HDH} system in tomato protoplasts encouraged us to explore co-editing at multiple sites. To this end, we selected three sites, *SlMYBATV*-cR, *SlGGP1*-cR, and *SlCYCB*-cR, for multiplexed editing, based on the Mb3Cas12a-RRR STU^{HDH} system (Figure 8d). Through *Agrobacterium*-mediated stable transformation, 25 transgenic plants were randomly selected for assessing the editing efficiencies of the three sites. Through Sanger sequencing and analysis, we found that the editing efficiencies at *SlMYBATV*-cR, *SlGGP1*-cR, and *SlCYCB*-cR sites are 8.0%, 12.0%, and 16.0%, respectively. The biallelic efficiency at three sites were 0%, 12.0%, and 4.0%, respectively (Figure 8e). The co-editing efficiency of three genes was 4.0%, and the co-editing efficiency of two genes was 12.0% (Figure 8f). We focused on 4 multiplex editing plants (481-5, 481-10, 481-11, and 481-16) for further analysis and all of them were edited at the *SlCYCB*-cR3 site (Figure 8g). Recently, a study showed that lycopene content increased when *SlCYCB* was knocked out in tomato (Arruabarrena *et al*., 2023). Thus, we recorded the phenotype of fruits at the breaker stage (Br) and 10 days after the breaker (Br + 10) stage (Figure 8h). Quantification of lycopene content indeed

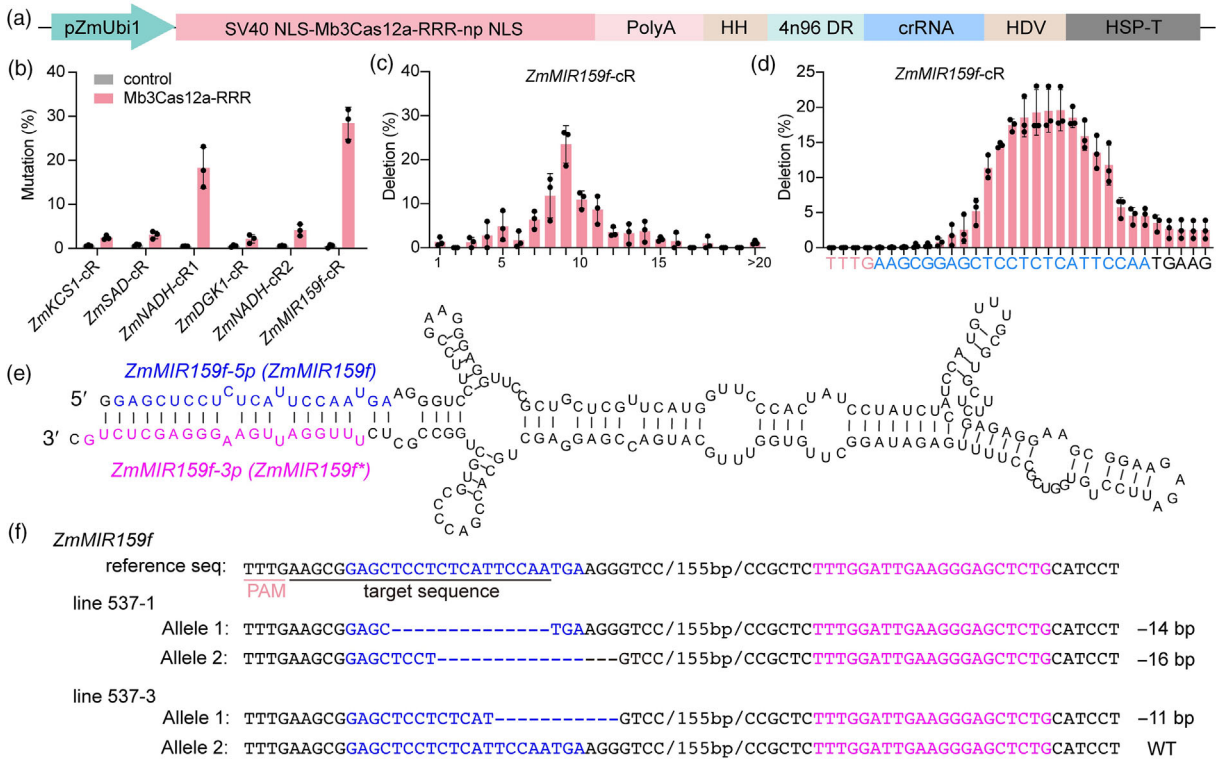

Figure 7 Application of the optimized CRISPR-Mb3Cas12a-RRR STU^{HDH} system for genome editing in maize. (a) Schematic of optimized Mb3Cas12a-RRR STU^{HDH} system for maize genome editing. 4n96 DR, 4n96 direct repeat; HDV, hepatitis delta virus ribozyme; HH, hammerhead ribozyme; HSP-T, heat shock protein terminator; np NLS, nucleoplasmin nuclear localization signal; pZmUbi, maize ubiquitin promoter. (b) Editing efficiencies of Mb3Cas12a-RRR system at six sites in maize protoplasts at 28 °C. Protoplasts transformed with the vector backbone were used as the control. (c) Deletion size profile of Mb3Cas12a-RRR variant at a representative target site in maize. (d) Deletion position profile of Mb3Cas12a-RRR variant at a representative target site in maize. PAM and spacer were colour-coded in red and blue, respectively. For experiments in maize protoplasts, three biological replicates were used. The error bars denote standard deviations. (e) RNAfold predicts stem-loop structure of *ZmMIR159f* primary microRNA (pri-miRNA) transcripts. The mature miRNA and its complementary strand (miRNA*) were colour-coded in blue and pink, respectively. (f) Genotypes of two T_0 plants with the *ZmMIR159f*-crR site edited by Mb3Cas12a-RRR. PAM and target sequence were underlined with red and black, respectively; the mature miRNA and miRNA* were colour-coded in blue and pink, respectively. For experiments in maize protoplasts, three biological replicates were used. The error bars denote standard deviations.

showed that the biallelic knockout plant (481-16) had significantly increased lycopene content in mature fruits (Figure 8i). Interestingly, intermediate increase of lycopene content was observed in all three monoallelic mutants, suggesting a gene dosage effect or haploid insufficiency (Figure 8i). Taken together, the Mb3Cas12a-RRR based STU^{HDH} system can achieve multiplexed editing in tomato.

Discussion

The CRISPR-Cas systems offer remarkable versatility and simplicity for crop breeding and trait engineering. Among the various CRISPR-Cas systems, CRISPR-Cas9 and Cas12a have emerged as the most widely utilized systems in plants. While CRISPR-Cas9 mediated genome editing has been extensively employed in plants, the commonly used SpCas9 recognized NGG PAM, limiting its targeting scope to GC rich regions. In contrast, CRISPR-Cas12a is increasingly gaining prominence in genome engineering due to its T-rich PAM recognition, ability to produced larger deletions, and versatile crRNA processing strategies for multiplexed editing (Zetsche *et al.*, 2015). Recently, multiple Cas12a orthologs have been identified and utilized for genome editing in plants, such as AsCas12a (Tang *et al.*, 2017), LbCas12a (Hu *et al.*, 2017; Tang *et al.*, 2017; Wang *et al.*, 2017), FnCas12a (Endo *et al.*, 2016; Zhong *et al.*, 2018), ErCas12a (MAD7) (Lin *et al.*, 2021), Mb2Cas12a (Zhang *et al.*, 2021b), Ev1Cas12a (Li *et al.*, 2023) and Hs1Cas12a (Li *et al.*, 2023). However, most of these Cas12a orthologs only recognized the canonical TTTV PAMs, necessitating the continued efforts to search for Cas12a orthologs and variants that can perform well at relaxed VTTV PAM sites. In this study, we compared three Cas12a orthologs (Mb3Cas12a, PrCas12a, and HkCas12a) and successfully identified Mb3Cas12a as a superior Cas12a ortholog with notable editing efficiency at NTTV PAM sites. Impressively, our data in rice showed that Mb3Cas12a overall exhibited more robust editing than that of FnCas12a and Mb2Cas12a (Figure 1c,d), both of which were previously preferred Cas12a orthologs for editing at VTTV PAM sites.

The STU system possesses a simple and compact configuration, utilizing only a Pol II promoter for the expression of Cas protein and guide RNA. This system offers the advantage of avoiding the use of Pol III promoters, which are not well characterized in many organisms and are more suitable for expressing short transcripts. Hence, the STU system has great potential for CRISPR-Cas

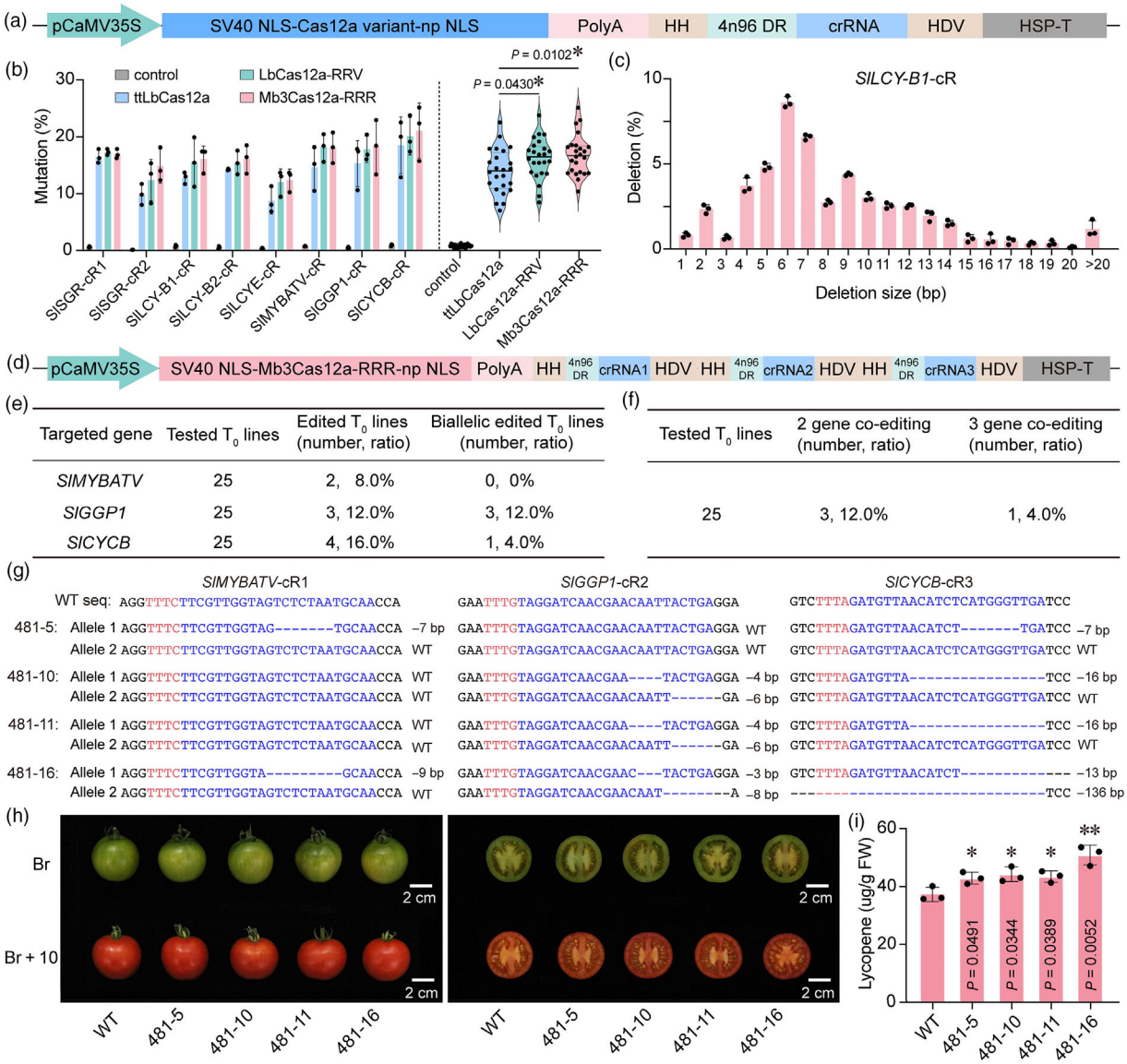

Targeted gene	Tested T_0 lines	Edited T_0 lines (number, ratio)	Biallelic edited T_0 lines (number, ratio)
SlMYBATV	25	2, 8.0%	0, 0%
SlGGP1	25	3, 12.0%	3, 12.0%
SlCYCB	25	4, 16.0%	1, 4.0%

Tested T_0 lines	2 gene co-editing (number, ratio)	3 gene co-editing (number, ratio)
25	3, 12.0%	1, 4.0%

Figure 8 Efficient multiplexed editing in tomato by the optimized CRISPR-Mb3Cas12a-RRR STU^{HDH} system. (a) Schematic of the optimized STU^{HDH} system for expressing different CRISPR-Cas12a systems for tomato genome editing. 4n96 DR, 4n96 direct repeat; Cas12a variant, ttLbCas12a, LbCas12a-RRV, and Mb3Cas12a-RRR; HDV, hepatitis delta virus ribozyme; HH, hammerhead ribozyme; HSP-T, heat shock protein terminator; np NLS, nucleoplasmin nuclear localization signal; pCaMV35S, cauliflower mosaic virus (CaMV) 35S promoter. (b) Comparison of editing efficiencies of ttLbCas12a, LbCas12a-RRV, and Mb3Cas12a-RRR systems at eight target sites in tomato protoplasts at 25 °C. Protoplasts transformed with the backbone vector were used as the control. (c) Deletion sizes profile of Mb3Cas12a-RRR at a representative target site in tomato. For experiments in tomato protoplasts, three biological replicates were used. The error bars denote standard deviations. (d) Schematic of multiplexed editing of three target sites by Mb3Cas12a-RRR in tomato. (e) Summary of total editing and biallelic editing efficiencies at three sites in transgenic tomato T_0 lines. (f) Further analysis of the data in "e" for co-editing efficiencies. (g) Sanger sequencing-based genotyping of four edited tomato T_0 lines. PAM and spacer were colour-coded in red and blue, respectively. (h) Image of tomato fruits from the four edited plants along with WT at breaker (Br) stage and 10 days after breaker (Br + 10) stage. Scale bar of fruit, 1 cm. (i) Lycopene content of ripe fruits in the four edited lines along with WT. Three biological replicates were used. The error bars denote standard deviations. Asterisks were used to denote statistical significance by Student's *t*-test (*$P < 0.05$; **$P < 0.01$).

mediated multiplexed genome editing (Tang *et al.*, 2016, 2019, 2024). In this study, we have developed a STU genome editing system based on Mb3Cas12a by incorporating HH and HDV ribozymes for crRNA processing. This STU^{HDH} system showed comparable editing efficiency to the efficient Dual Pol II system (Zhang *et al.*, 2021b) (Figure 3). Interestingly, our data showed that self-processing of the DR array by Mb3Cas12a showed poor activity (Figure S3), suggesting Mb3Cas12a may not have an optimal activity in self-processing of its crRNA array. By contrast, the Mb3Cas12a STU^{HDH} system based on the HH-HDV dual-ribozyme system showed high editing activities, consistent with our previous results on comparison of the HH-HDV system and the DR array system (Tang *et al.*, 2017, 2024; Zhang *et al.*, 2021b). Regardless, it is important to significantly improve the Mb3Cas12a STU genome editing systems in plants, which is the major focus of this study.

We further developed the Mb3Cas12a-STU^{HDH} system by optimizing key elements such as the linker between Mb3Cas12a and crRNA, NLS configuration, crRNA structure, and Mb3Cas12a protein structure. First, we compared three linkers, PolyA, Triplex, and Comp.14. In contrast to mammalian cells, our results indicated that the PolyA terminator is better suited for the STU system in plants (Figure 4a,b). Next, we compared three NLS structures, NC NLS, 3C NLS, and 2C NLS. The 3C NLS structure has shown efficient editing activities in Cas9 (Fan *et al*., 2024; Li *et al*., 2020; Zhong *et al*., 2023), while the 2C NLS structure has demonstrated efficient editing activities in Cas12a in mammalian cells (Liu *et al*., 2019). However, our findings revealed that the NC NLS structure is more efficient than these two NLS configurations in plants (Figure 4c,d). Our data suggested that different CRISPR-Cas systems require different optimization strategies, which may differ between mammals and plants. Additionally, we compared six DR structures (4n61, 4n91, 4n96, 4n128, 4n137, and 4n149), and identified the 4n96 DR to be the most efficient one for both Mb3Cas12a and FnCas12a, even surpassing these Cas12a nucleases' own DR structures (Figure 4e,f and Figure S5). These results suggested that 4n96 DR may be suitable for diverse Cas12a orthologs, which however warrants future investigations. We applied our optimized Mb3Cas12a STU^{HDH} (Mb3Cas12a with NC NLS, polyA, and 4n96 DR) system for multiplexed promoter editing in rice. By editing the promoters of *OsGBSS1* (Figure 5) and *OsD18* (Figure 6), quantitative trait variations in amylose content and semi dwarfism were efficiently introduced, highlight the great potential of this Mb3Cas12a STU^{HDH} system for crop improvement, considering that Mb3Cas12a has superior activity at editing relaxed VTTV PAM sites than many other Cas12a orthologs.

Cas12a nucleases have shown sensitivity to lower temperatures (Malzahn *et al*., 2019), which is a significant factor limiting their application in diverse plants. Several studies have shown that the activities of Cas12a can be improved through protein engineering (e.g., enAsCas12a (Kleinstiver *et al*., 2019) and ttLbCas12a (Schindele and Puchta, 2020)) and directed evolution (e.g., AsCas12a Ultra (Zhang *et al*., 2021a), LbCas12a-RRV (Zhang *et al*., 2023)). In this study, we engineered two temperature-tolerant variants, Mb3Cas12a-R and Mb3Cas12a-RRR (Figure S6). The editing efficiencies of these variants were comparable to that of Mb3Cas12a at 32 °C in rice protoplasts. This suggests that all these nucleases, when combined with the NC NLS, polyA, and 4n96 DR, are suitable options for monocots, such as rice, at 32 °C. However, the variants, particularly Mb3Cas12a-RRR, exhibited higher editing activities at lower temperatures (28 °C and 22 °C) (Figure 4h). Leveraging the promising editing efficiency of Mb3Cas12a-RRR at lower temperatures, we demonstrated its application for genome editing in maize, by knocking out a non-coding miRNA gene *ZmMIR159f* (Figure 7e,f). We further tested Mb3Cas12a-RRR in tomato, a dicot plant. In this case, we benchmarked Mb3Cas12a-RRR against ttLbCas12a (Schindele and Puchta, 2020) and LbCas12a-RRV (Zhang *et al*., 2023), both of which represent the most efficient Cas12a nucleases ever engineered for genome editing in plants. Impressively, Mb3Cas12a-RRR showed comparable genome editing efficiency to LbCas12a-RRV and more robust genome editing efficiency than ttLbCas12a in tomato protoplasts (Figure 8b). Subsequently, Mb3Cas12a-RRR was demonstrated to achieve multiplexed genome editing of *SlMYBATV*, *SlGGP1*, and *SlCYCB* in stable tomato plants (Figure 8d–g). This suggests that our optimized Mb3Cas12a-RRR STU system (with NC NLS, polyA, and 4n96 DR), is suitable for genome editing in both monocots and dicots in a wide range of temperature conditions.

Conclusion

By taking a stepwise approach to systematically optimize different factors, we have successfully developed an efficient Mb3Cas12a STU^{HDH} system with optimized linker, NLS configuration, crRNA expression and processing, crRNA structure, and protein engineering. The improved Mb3Cas12a-RRR STU^{HDH} system (Mb3Cas12a-RRR nuclease combined with NC NLS, polyA, and 4n96 DR) confers robust and temperature-tolerant multiplexed genome editing in rice, maize, and tomato. We demonstrated the use of such systems for promoter editing to engineer quantitative traits in rice, for knocking out a non-coding gene in maize, and for enhancing lycopene content in tomato fruits. It is expected a wide range of applications can be realized by using this CRISPR-Cas12a system in diverse plant species.

Experimental procedures

Construction of the vectors

The rice codon optimized PrCas12a, HkCas12a and Mb3Cas12a were synthesized by GenScript (Nanjing, China) and cloned in pMOD_A (pZmUbi1-ccdB-HSP T) vector using Golden Gate assembly to construct the module-A vectors: pYSS120 (PrCas12a), pYSS118 (HkCas12a), and pLSS62 (Mb3Cas12a), respectively. The mature crRNA repeats of PrCas12a, HkCas12a and Mb3Cas12a were synthesized by overlapping extension PCR, and then assembled into the vector containing pOsUbi1-HH-HDV-pinII T using Gibson assemble to construct the module-B vectors: pLSS02 (PrCas12a mature crRNA repeats), pLSS22 (HkCas12a mature crRNA repeats), and pLSS21 (Mb3Cas12a mature crRNA repeats), respectively. The vectors of module-A, module-B and pMOD_C0000a were assembled into the T-DNA backbone vector pTRANS_210d (Addgene Plasmid #91109) (Cermak *et al*., 2017) using Golden Gate assembly to generate T-DNA vectors pGEL1022 (HkCas12a, Addgene Plasmid #225593), pGEL1023 (PrCas12a, Addgene Plasmid #225594), and pGEL1024 (Mb3Cas12a, Addgene Plasmid #225595). The coding sequences of HkCas12a, PrCas12a, and Mb3Cas12a were provided in Figure S11. The editing vectors were generated by annealing two synthesized oligonucleotides flanked with *Bsa*I restriction enzyme sites. The final T-DNA recombinant expression vectors were constructed using Golden Gate assembly.

For making Mb3Cas12a-STU^{HDH} systems, we amplified Mb3Cas12a and polyA-ccdB-DR fragments from pGEL1024 and pGEL032 (Tang *et al*., 2019) respectively and replaced the fragment of LbCas12a and its DR from pGEL032 using *Sbf*I (Thermo Fisher scientific, catalogue FD1194) and *Xba*I (Thermo Fisher scientific, catalogue FD0684) to construct vector pLSS375. The linkers, Triplex (Campa *et al*., 2019) and Comp.14 (Wilusz *et al*., 2012) were synthesized by GenScript (Nanjing, China) and then cloned into pLSS375 vector linearized by *Xma*I (Thermo Fisher scientific, catalogue ER0171), with a partial fragment of Mb3Cas12a using Gibson assembly. The linker sequences were provided in Figure S12. The 3C NLS and 2C NLS were synthesized by Sangon biotech (Shanghai, China) and then cloned into pLSS375-*Sbf*I + *Srf*I (NEB, catalogue R0629S) using Gibson assembly. The NLS sequences were provided in Figure S13. The DR sequences (4n61, 4n91, 4n96, 4n128, 4n137 and 4n149) were synthesized by Sangon biotech, and cloned into pLSS375-*Kpn*I

(Thermo Fisher scientific, catalogue FD0524) + *Bst*XI (Thermo Fisher scientific, catalogue FD1024) using Gibson assembly. The DR sequences were provided in Figure 4e. To prepare the Mb3Cas12a-R variant (pGEL1026, Addgene Plasmid #225597), the D172R mutation was introduced into pGEL1025 (Mb3Cas12a with 4n96 DR, Addgene Plasmid #225596) with mutagenesis PCR. Mb3Cas12a-R fragment was introduced into the *Sbf*I and *BsmB*I (Thermo Fisher scientific, catalogue ER0451) digested T-DNA vector pGEL1025 using Gibson assembly. The construction of Mb3Cas12a-RRR variant (pGEL1027, Addgene Plasmid #225598) is similar to Mb3Cas12a-R, the three mutations (D172R/N573R/K579R) were introduced into pGEL1025 with mutagenesis PCR. Mb3Cas12a-RRR fragment was introduced into the *Sbf*I and *BsmB*I digested T-DNA vector pGEL1025 using Gibson assembly. The Mb3Cas12a-RVRR variant was constructed similarly. Mutagenesis PCR was used to amplify the four mutations (N573R/K579V/N583R/K635R) and then the PCR product was cloned into the *Sbf*I and *BsmB*I digested T-DNA vector pGEL1025 using Gibson assembly. The coding sequences of Mb3Cas12a-R, Mb3Cas12a-RRR, Mb3Cas12a-RVRR were provided in Figure S11. The pGEL1028 (Addgene Plasmid #225599) containing ZmUbi1 promoter was used for Mb3Cas12a-RRR expression in maize. The pGEL1029 (Addgene Plasmid #225600) containing CaMV35S promoter was used for Mb3Cas12a-RRR expression in tomato. The resulting vectors were confirmed by Sanger sequencing. Tables S1–S3 provides a comprehensive list of the oligos, T-DNA vectors, and crRNAs used in this study, respectively.

Rice protoplast transformation and stable transformation

The rice cultivar *Nipponbare* (*Oryza sativa* L. japonica) was used in this study. For rice protoplast transformation, a previous protocol was followed (He *et al*., 2024; Liu *et al*., 2022; Tang *et al*., 2020). Briefly, rice seedlings were cultivated for 11 days in darkness at 28 °C. Subsequently, leaf segments approximately 1.0 mm in length were excised and immersed in the enzyme digestion solution, followed by vacuum infiltration for 30 min. The treated leaf strips were then subjected to incubation at 25 °C in darkness, with agitation at 70–80 rpm, for a period ranging between 6 and 8 h. Post-digestion, the mixture underwent filtration using a 40 μm cell strainer, thereby isolating the protoplasts. The protoplast suspension was centrifuged at 100 g for 5 min, after which the supernatant was discarded, and the protoplasts were re-suspended in W5 buffer. Following decantation of the W5 buffer, protoplasts were re-suspended at a concentration of 2×10^6/mL in MMG solution. Subsequently, a mixture comprising 30 μg of T-DNA plasmid and MMG was prepared, constituting a total volume of 30 μL, and introduced into 200 μL of protoplasts (4×10^5 protoplasts). This mixture was subjected to 30 min incubation in a PEG solution of equal volume. The transfection mixture was subsequently diluted with 1 mL of W5 buffer and centrifuged at 250 g for 5 min to eliminate the supernatant. The protoplasts were gently resuspended in W5 buffer and distributed evenly into individual wells of a 12-well tissue culture plate. Following an incubation period of 48 h at 32 °C in darkness, the protoplasts were harvested for subsequent genome editing analyses. For analysing the editing activity of Mb3Cas12a and its variants at different temperatures, the protoplasts were incubated for 48 h at 22 °C, 28 °C, and 32 °C in the incubator in darkness respectively after protoplast transformation. Then the protoplasts were harvested for subsequent genome editing analyses.

Transgenic rice lines were prepared using *Agrobacterium*-mediated transformation which was conducted as published previously (Toki *et al*., 2006; Zheng *et al*., 2023). Briefly, rice calli were induced from seeds and cultured on N6-D medium for 7 days at 32 °C under light conditions. The T-DNA vectors were introduced into *Agrobacterium tumefaciens* strain EHA105 by freeze–thaw transformation. Each transformed *Agrobacterium* EHA105 culture was incubated at 28 °C and then resuspended in AAM-AS medium (OD_{600} = 0.1) supplemented with 100 mM acetosyringone (AS). Following a 3-day co-cultivation period with *Agrobacterium*, the calli were washed with sterile water and transferred to N6-S medium containing 200 mg/L timentin and 50 mg/L hygromycin, where they were incubated for 2 weeks. Subsequently, resistant calli were transferred to REIII medium supplemented with 200 mg/L timentin and 50 mg/L hygromycin to facilitate plant regeneration.

Maize protoplast transformation and stable transformation

The maize cultivar Xiang 249 (X249) was used in this study. For maize protoplast transformation, the process is similar to that used for rice with some optimization (He *et al*., 2024; Liu *et al*., 2022; Tang *et al*., 2020). Briefly, the maize seedlings were cultivated for 10 days in darkness at 28 °C. Subsequently, leaves were cut to about 1.0 mm strips and transferred into the enzyme solution (the same as that used for rice) followed by vacuum-infiltration for 30 min. The treated leaf strips were then subjected to incubation at 25 °C in darkness, with agitation at 50–70 rpm, for a period ranging between 6 and 8 h. Post-digestion, each digestion mixture was filtered using a 40 μm cell strainer to collect the protoplasts. The protoplasts were centrifuged at 100 g for 5 min, after which the supernatant was discarded, and the protoplasts were re-suspended in W5 buffer. Upon introduced of the W5 buffer, protoplasts were diluted at a concentration of 2×10^6/mL in MMG solution. Following this, a mixture comprising 30 μg of T-DNA plasmid and MMG was meticulously prepared, amounting to a total volume of 30 μL, and subsequently introduced into 200 μL of protoplasts (4×10^5 protoplasts). This mixture underwent a 30-min incubation period in a PEG solution of equivalent volume. Subsequently, the transfection mixture was diluted with 1 mL of W5 buffer and subjected to centrifugation at 250 g for 5 min to facilitate removal of the supernatant. The protoplasts were resuspended in W5 buffer and evenly dispensed into individual wells of a 12-well tissue culture plate. Following an incubation duration of 48 h at 28 °C in the absence of light, the protoplasts were collected for subsequent genome editing analyses.

The genetic stable transformation of maize was conducted according to the method reported with some optimization (Wei, 2009). For the genetic transformation process of maize, immature embryos from the self-pollinated X249 line were excised when the seeds were pollinated for 8–12 days, and the immature embryos reached a length of approximately 0.8–1.8 mm. The sterilized immature embryos were put into a 2 mL tube containing liquid XI infection medium with acetosyringone (AS). About 100 immature embryos were collected in each 2.0 mL tube. Before infection, XI infection medium was used to wash the isolated immature embryos. Then the immature embryos were immersed in 1 mL of *Agrobacterium tumefaciens* culture (OD_{600} = 0.3). After thorough mixing for 30 s, the immature embryos were subjected to incubation for 5 min in dark. After infection, the immature embryos were transferred

along with the bacterial suspension onto co-cultivation medium. Gentle agitation of the culture dish was applied to ensure even distribution of the immature embryos on the medium. Afterwards, the immature embryos were delicately flipped using sterile forceps, with the round side facing upwards and the flat side downwards. Subsequently, they were subjected to dark incubation at 23 °C for 2 days. After 2 days of co-cultivation, the immature embryos were transferred to XR medium using sterile forceps, followed by dark incubation at 28 °C for approximately 7 days. Upon completion of resting medium incubation, immature embryos were transferred to selection medium I containing bialaphos (5 mg/L). Incubation was carried out in darkness at 28 °C for 14–18 days. Calli masses derived from individual immature embryos were dissected along the natural growth fissures of the resistant callus using forceps, yielding approximately 5 mm diameter pieces. Each callus mass originating from a single immature embryo was considered a unit. These callus masses were then transferred to selection medium II containing bialaphos at 8 mg/L and incubated in darkness at 28 °C for 14 days. Upon completion of the selection phase, resistant calli were transferred to differentiation medium I supplemented with bialaphos at 3 mg/L and cultured at 25 °C under a light intensity of 5000 lux with a photoperiod of 16 h per day for 7 days. Once calli or shoots turned green, they were promptly transferred to differentiation medium II and cultured at 25 °C under a light intensity of 5000 lux with a photoperiod of 16 h per day for 14 days to obtain regenerated seedlings. Healthy regenerated seedlings with main stems were transferred to the rooting medium and cultured at 25 °C under a light intensity of 5000 lux with a photoperiod of 16 h per day for 7–14 days. After root formation, partial leaf tissue of each seedling was taken for DNA extraction and targeted mutation analysis.

Tomato protoplast transformation and stable transformation

The Alisa Craig cultivar of tomato was used in this study. For tomato protoplast transformation, a previous protocol was followed (Fan *et al*., 2024; Liu *et al*., 2022). Briefly, the tomato plants were cultivated under controlled conditions at 25 °C with a photoperiod of 12 h light and 12 h dark. Leaves were cut to 1 mm from 25- to 30-day old plants. The leaves were subsequently subjected to enzymatic digestion in a solution maintained at 25 °C in darkness for a duration of 10–12 h. Following digestion, the resulting cellular suspension was sieved through a 75 μm cell strainer pre-soaked with W5 buffer and subsequently centrifuged at 200 g for 10 min. The supernatant was meticulously removed, and the cells were resuspended in a solution containing 0.55 M sucrose. Upon centrifugation at 200 g for 30 min, a distinct band of protoplasts formed at the interface, which were then carefully transferred to new 10 mL tubes and subjected to two washes with 10 mL of W5 buffer. The protoplasts were then resuspended in MMG solution, and the final concentration was adjusted to 5×10^5/mL. Subsequently, a gentle mixing of 20 μL of plasmid DNA (at a concentration of 1500 ng/μL), 200 μL of protoplasts, and 220 μL of filter-sterilized 40% PEG solution was carried out in a 2 mL round tube. Following a 30-min incubation period at room temperature, the reactions were halted by the addition of 1000 μL of W5 buffer. The protoplasts were harvested via centrifugation and subsequently transferred into 12-well culture plates. These plates were then incubated at 25 °C in darkness for a duration of 48 h.

For the genetic transformation process of tomato, seeds were disinfected with a 5% sodium hypochlorite solution for 15 min, followed by rinsing with sterile water three times, and sown in 1/2MS medium. The plants were grown in sterile conditions in a culture chamber with controlled temperatures of 22 °C/18 °C and a photoperiod of 16 h/8 h (day/night) for 6–7 days. The cotyledons were fully expanded and used for *Agrobacterium*-mediated transformation. The genetic transformation of tomato was conducted according to the method reported with optimization (Van Eck *et al*., 2019). Firstly, the middle portion of the cotyledons was placed on pre-culture medium KCMS for 1 day. Secondly, the *Agrobacterium* infiltration solution was prepared with an OD_{600} = 0.1, and the cotyledons were infiltrated for 20 min, followed by removal of the bacterial liquid and incubation in the dark for 2 days. Thirdly, the cotyledons were then transferred to selection medium (MS salt 4.4 g/L + sucrose 30 g/L + agar 8 g/L + organic 1 mL/L + Zeatin 2 mg/L + Augmentin 400 mg/L + Timentin 200 mg/L + Kanamycin 100 mg/L, pH 5.8) and the medium was replaced every 3–4 weeks for subculture. Finally, the resistant callus was carefully excised and transferred to rooting medium (MS salt 4.4 g/L + sucrose 30 g/L + agar 8 g/L + organic 1 mL/L + Augmentin 200 mg/L + Timentin 100 mg/L + Kanamycin 50 mg/L, pH 5.8) for root induction. When the tomato seedlings grew into adult plants, the leave were used for mutation analysis.

Detection of targeted mutations

The protoplasts or leave derived from rice, maize, or tomato were subjected to DNA extraction utilizing the CTAB method (Stewart Jr. and Via, 1993). Targeted mutagenesis quantification of protoplasts was carried out through next-generation sequencing (NGS) of polymerase chain reaction (PCR) amplicons amplified with barcoded primers. After sequencing, data analysis was executed employing CRISPRMatch (You *et al*., 2018) and CrisprStitch (Han *et al*., 2024). Genotyping of T_0 or T_1 lines were sequenced by Sanger sequencing of PCR amplicons. The sequencing data were analysed using the CRISPR-GE DSDecodeM software (Xie *et al*., 2017).

Investigation on agronomic characters of rice

The rice cultivar *Nipponbare* (*Oryza sativa* L. japonica) was used as the WT control, the promoter editing lines and WT lines were conducted at Chengdu, Sichuan province (30° 43′ N, 103° 52′ E) in 2023 in natural environments. The rice yield-related traits were measured according to a previous method (Shen *et al*., 2018). Eight to ten individual plants were used for data collection of each genotype. The total starch content and amylose content were measured in Shanghai Sanshu Biotechnology Company.

Iodine staining of endosperm

The hulls of rice seeds were removed to observe phenotypes of the grains. The grains were dissected longitudinally to expose the endosperm. Then the solution of iodine reagent (0.2%) was dropped onto these gains, and images were captured following an incubation period of 3–5 min (Zheng *et al*., 2018).

RNA extraction and RT-qPCR

For *OsGBSS1* promoter editing plants, panicles were collected at 7 days post-flowering to extract RNA. For *OsD18* promoter editing plants, leaves from the 60 day-old plants were collected to extract RNA. RNA extraction was performed using the SteadyPure Plant RNA Isolation Kit (Accurate Biology, China),

followed by reverse transcription using the HiScript III 1st Strand cDNA Synthesis Kit (Vazyme, China). Real-time quantitative polymerase chain reaction (qPCR) was conducted using the ChamQ Universal SYBR qPCR Master Mix (Vazyme, China) following the manufacturer's instructions, with *OsActin* used as control. The $2^{-\Delta\Delta Ct}$ method was used to calculate the relative expression levels of the target genes. Three biological replicates were used in this analysis. The primers used in qPCR are listed in Table S1.

Data analysis

All data were analysed with the GraphPad Prism 9.0 software, and the figures were made using the Adobe Photoshop and Adobe Illustrator software.

Acknowledgements

This research was supported by the Biological Breeding-Major Projects (2023ZD04074) and the National Key Research and Development Program of China (award no. 2023YFD1202900) to Y.Z. and X.T., the National Natural Science Foundation of China (award no. 32270433, 32101205 and 32072045) to Y.Z., X.T., and X.Z. It is also supported by the NSF Plant Genome Research Program (IOS-2029889 and IOS-2132693) to Y.Q.

Author contributions

Y.Z. designed the experiments. S.L. and Y.H. designed and made the constructs. S.L., Y.H., M.Y. and X.T. generated all T-DNA vectors. S.L., Y.H., and Z.Z. conducted rice protoplast isolation and transformation. S.L. did rice NGS samples preparation and data analysis. S.L., Y.H., T.F. and J.Z. conducted stable transformation of rice and analysis of editing. S.L. did the tomato protoplast transformation and NGS analysis of editing. C.Q., Y.M. and L.Y. conducted stable transformation of tomato. S.L. did the maize protoplast transformation and NGS analysis of editing. M.Z. and X.A. conducted stable transformation of maize. Y.Z., Y.Q., and S.L. analysed the data and wrote the manuscript. All authors participated in discussion and revision of the manuscript.

Conflict of interest

The authors declare no competing interests.

Data availability statement

The raw data of deep sequencing have been deposited to the Sequence Read Archive in National Center for Biotechnology Information (NCBI) under the accession number PRJNA1099330.

References

Alfatih, A., Wu, J., Jan, S.U., Zhang, Z.S., Xia, J.Q. and Xiang, C.B. (2020) Loss of rice PARAQUAT TOLERANCE 3 confers enhanced resistance to abiotic stresses and increases grain yield in field. *Plant Cell Environ.* **43**, 2743–2754.

Arruabarrena, A., Lado, J., Gonzalez-Arcos, M. and Vidal, S. (2023) Targeted disruption of tomato chromoplast-specific lycopene beta-cyclase (CYC-B) gene promotes early accumulation of lycopene in fruits and enhanced postharvest cold tolerance. *Plant Biotechnol. J.* **21**, 2420–2422.

Bernabe-Orts, J.M., Casas-Rodrigo, I., Minguet, E.G., Landolfi, V., Garcia-Carpintero, V., Gianoglio, S., Vazquez-Vilar, M. *et al.* (2019) Assessment of Cas12a-mediated gene editing efficiency in plants. *Plant Biotechnol. J.* **17**, 1971–1984.

Campa, C.C., Weisbach, N.R., Santinha, A.J., Incarnato, D. and Platt, R.J. (2019) Multiplexed genome engineering by Cas12a and CRISPR arrays encoded on single transcripts. *Nat. Methods*, **16**, 887–893.

Cermak, T., Curtin, S.J., Gil-Humanes, J., Cegan, R., Kono, T.J.Y., Konecna, E., Belanto, J.J. *et al.* (2017) A multipurpose toolkit to enable advanced genome engineering in plants. *Plant Cell*, **29**, 1196–1217.

Dong, O.X., Yu, S., Jain, R., Zhang, N., Duong, P.Q., Butler, C., Li, Y. *et al.* (2020) Marker-free carotenoid-enriched rice generated through targeted gene insertion using CRISPR-Cas9. *Nat. Commun.* **11**, 1178.

Endo, A., Masafumi, M., Kaya, H. and Toki, S. (2016) Efficient targeted mutagenesis of rice and tobacco genomes using Cpf1 from *Francisella novicida*. *Sci. Rep.* **6**, 38169.

Eshed, Y. and Lippman, Z.B. (2019) Revolutions in agriculture chart a course for targeted breeding of old and new crops. *Science*, **366**, eaax0025.

Fan, T., Cheng, Y., Wu, Y., Liu, S., Tang, X., He, Y., Liao, S. *et al.* (2024) High performance TadA-8e derived cytosine and dual base editors with undetectable off-target effects in plants. *Nat. Commun.* **15**, 5103.

Fu, Z.W., Li, J.H., Gao, X., Wang, S.J., Yuan, T.T. and Lu, Y.T. (2024) Pathogen-induced methylglyoxal negatively regulates rice bacterial blight resistance by inhibiting OsCDR1 protease activity. *Mol. Plant*, **17**, 325–341.

Gao, L., Cox, D.B.T., Yan, W.X., Manteiga, J.C., Schneider, M.W., Yamano, T., Nishimasu, H. *et al.* (2017) Engineered Cpf1 variants with altered PAM specificities. *Nat. Biotechnol.* **35**, 789–792.

Han, Y., Liu, G., Wu, Y., Bao, Y., Zhang, Y. and Zhang, T. (2024) CrisprStitch: fast evaluation of the efficiency of CRISPR editing systems. *Plant Commun.* **5**, 100783.

He, Y., Han, Y., Ma, Y., Liu, S., Fan, T., Liang, Y., Tang, X. *et al.* (2024) Expanding plant genome editing scope and profiles with CRISPR-FrCas9 systems targeting palindromic TA sites. *Plant Biotechnol. J.* **22**, 2488–2503.

Hu, X., Wang, C., Liu, Q., Fu, Y. and Wang, K. (2017) Targeted mutagenesis in rice using CRISPR-Cpf1 system. *J. Genet. Genomics*, **44**, 71–73.

Hu, S., Hu, X., Hu, J., Shang, L., Dong, G., Zeng, D., Guo, L. *et al.* (2018) Xiaowei, a new rice germplasm for large-scale indoor research. *Mol. Plant*, **11**, 1418–1420.

Huang, Y., Cao, H., Yang, L., Chen, C., Shabala, L., Xiong, M., Niu, M. *et al.* (2019) Tissue-specific respiratory burst oxidase homolog-dependent H_2O_2 signaling to the plasma membrane H+-ATPase confers potassium uptake and salinity tolerance in Cucurbitaceae. *J. Exp. Bot.* **70**, 5879–5893.

Huang, L., Sreenivasulu, N. and Liu, Q. (2020) Waxy editing: old meets new. *Trends Plant Sci.* **25**, 963–966.

Hui, F., Tang, X., Li, B., Alariqi, M., Xu, Z., Meng, Q., Hu, Y. *et al.* (2024) Robust CRISPR/Mb2Cas12a genome editing tools in cotton plants. *iMeta*, **3**, e209.

Jacobsen, T., Ttofali, F., Liao, C., Manchalu, S., Gray, B.N. and Beisel, C.L. (2020) Characterization of Cas12a nucleases reveals diverse PAM profiles between closely-related orthologs. *Nucleic Acids Res.* **48**, 5624–5638.

Jinek, M., Chylinski, K., Fonfara, I., Hauer, M., Doudna, J.A. and Charpentier, E. (2012) A programmable dual-RNA-guided DNA endonuclease in adaptive bacterial immunity. *Science*, **337**, 816–821.

Kim, D., Kim, J., Hur, J.K., Been, K.W., Yoon, S.H. and Kim, J.S. (2016) Genome-wide analysis reveals specificities of Cpf1 endonucleases in human cells. *Nat. Biotechnol.* **34**, 863–868.

Kleinstiver, B.P., Tsai, S.Q., Prew, M.S., Nguyen, N.T., Welch, M.M., Lopez, J.M., McCaw, Z.R. *et al.* (2016) Genome-wide specificities of CRISPR-Cas Cpf1 nucleases in human cells. *Nat. Biotechnol.* **34**, 869–874.

Kleinstiver, B.P., Sousa, A.A., Walton, R.T., Tak, Y.E., Hsu, J.Y., Clement, K., Welch, M.M. *et al.* (2019) Engineered CRISPR-Cas12a variants with increased activities and improved targeting ranges for gene, epigenetic and base editing. *Nat. Biotechnol.* **37**, 276–282.

Lee, K., Zhang, Y., Kleinstiver, B.P., Guo, J.A., Aryee, M.J., Miller, J., Malzahn, A. *et al.* (2019) Activities and specificities of CRISPR/Cas9 and Cas12a nucleases for targeted mutagenesis in maize. *Plant Biotechnol. J.* **17**, 362–372.

Li, R., Li, R., Li, X., Fu, D., Zhu, B., Tian, H., Luo, Y. *et al.* (2018) Multiplexed CRISPR/Cas9-mediated metabolic engineering of gamma-aminobutyric acid levels in *Solanum lycopersicum*. *Plant Biotechnol. J.* **16**, 415–427.

Li, C., Zong, Y., Jin, S., Zhu, H., Lin, D., Li, S., Qiu, J.L. *et al.* (2020) SWISS: multiplexed orthogonal genome editing in plants with a Cas9 nickase and engineered CRISPR RNA scaffolds. *Genome Biol.* **21**, 141.

Li, G., Zhang, Y., Dailey, M. and Qi, Y. (2023) Hs1Cas12a and Ev1Cas12a confer efficient genome editing in plants. *Front. Genome Ed.* **5**, 1251903.

Lin, Q., Zhu, Z., Liu, G., Sun, C., Lin, D., Xue, C., Li, S. *et al*. (2021) Genome editing in plants with MAD7 nuclease. *J. Genet. Genomics*, **48**, 444–451.

Liu, J., Chen, J., Zheng, X., Wu, F., Lin, Q., Heng, Y., Tian, P. *et al*. (2017) GW5 acts in the brassinosteroid signalling pathway to regulate grain width and weight in rice. *Nat. Plants*, **3**, 17043.

Liu, H., Soyars, C.L., Li, J., Fei, Q., He, G., Peterson, B.A., Meyers, B.C. *et al*. (2018) CRISPR/Cas9-mediated resistance to cauliflower mosaic virus. *Plant Direct*, **2**, e00047.

Liu, P., Luk, K., Shin, M., Idrizi, F., Kwok, S., Roscoe, B., Mintzer, E. *et al*. (2019) Enhanced Cas12a editing in mammalian cells and zebrafish. *Nucleic Acids Res.* **47**, 4169–4180.

Liu, X., Wu, D., Shan, T., Xu, S., Qin, R., Li, H., Negm, M. *et al*. (2020) The trihelix transcription factor OsGTgamma-2 is involved adaption to salt stress in rice. *Plant Mol. Biol.* **103**, 545–560.

Liu, L., Gallagher, J., Arevalo, E.D., Chen, R., Skopelitis, T., Wu, Q., Bartlett, M. *et al*. (2021) Enhancing grain-yield-related traits by CRISPR-Cas9 promoter editing of maize CLE genes. *Nat Plants*, **7**, 287–294.

Liu, S., Sretenovic, S., Fan, T., Cheng, Y., Li, G., Qi, A., Tang, X. *et al*. (2022) Hypercompact CRISPR-Cas12j2 (CasPhi) enables genome editing, gene activation, and epigenome editing in plants. *Plant Commun.* **3**, 100453.

Mahas, A., Aman, R. and Mahfouz, M. (2019) CRISPR-Cas13d mediates robust RNA virus interference in plants. *Genome Biol.* **20**, 263.

Malzahn, A.A., Tang, X., Lee, K., Ren, Q., Sretenovic, S., Zhang, Y., Chen, H. *et al*. (2019) Application of CRISPR-Cas12a temperature sensitivity for improved genome editing in rice, maize, and Arabidopsis. *BMC Biol.* **17**, 9.

Oliva, R., Ji, C., Atienza-Grande, G., Huguet-Tapia, J.C., Perez-Quintero, A., Li, T., Eom, J.S. *et al*. (2019) Broad-spectrum resistance to bacterial blight in rice using genome editing. *Nat. Biotechnol.* **37**, 1344–1350.

Peng, A., Chen, S., Lei, T., Xu, L., He, Y., Wu, L., Yao, L. *et al*. (2017) Engineering canker-resistant plants through CRISPR/Cas9-targeted editing of the susceptibility gene CsLOB1 promoter in citrus. *Plant Biotechnol. J.* **15**, 1509–1519.

Ren, Q., Sretenovic, S., Liu, G., Zhong, Z., Wang, J., Huang, L., Tang, X. *et al*. (2021a) Improved plant cytosine base editors with high editing activity, purity, and specificity. *Plant Biotechnol. J.* **19**, 2052–2068.

Ren, Q., Sretenovic, S., Liu, S., Tang, X., Huang, L., He, Y., Liu, L. *et al*. (2021b) PAM-less plant genome editing using a CRISPR-SpRY toolbox. *Nat. Plants*, **7**, 25–33.

Rodriguez-Leal, D., Lemmon, Z.H., Man, J., Bartlett, M.E. and Lippman, Z.B. (2017) Engineering quantitative trait variation for crop improvement by genome editing. *Cell*, **171**, 470–480.e478.

Sanchez-Leon, S., Gil-Humanes, J., Ozuna, C.V., Gimenez, M.J., Sousa, C., Voytas, D.F. and Barro, F. (2018) Low-gluten, nontransgenic wheat engineered with CRISPR/Cas9. *Plant Biotechnol. J.* **16**, 902–910.

Sasaki, A., Ashikari, M., Ueguchi-Tanaka, M., Itoh, H., Nishimura, A., Swapan, D., Ishiyama, K. *et al*. (2002) Green revolution: a mutant gibberellin-synthesis gene in rice. *Nature*, **416**, 701–702.

Schindele, P. and Puchta, H. (2020) Engineering CRISPR/LbCas12a for highly efficient, temperature-tolerant plant gene editing. *Plant Biotechnol. J.* **18**, 1118–1120.

Shen, L., Wang, C., Fu, Y., Wang, J., Liu, Q., Zhang, X., Yan, C. *et al*. (2018) QTL editing confers opposing yield performance in different rice varieties. *J. Integr. Plant Biol.* **60**, 89–93.

Song, X.J., Huang, W., Shi, M., Zhu, M.Z. and Lin, H.X. (2007) A QTL for rice grain width and weight encodes a previously unknown RING-type E3 ubiquitin ligase. *Nat. Genet.* **39**, 623–630.

Stewart, C.N., Jr. and Via, L.E. (1993) A rapid CTAB DNA isolation technique useful for RAPD fingerprinting and other PCR applications. *Biotechniques*, **14**, 748–750.

Su, H., Cao, L., Ren, Z., Sun, W., Zhu, B., Ma, S., Sun, C. *et al*. (2023) ZmELF6-ZmPRR37 module regulates maize flowering and salt response. *Plant Biotechnol. J.* **22**, 929–945.

Tang, X. and Zhang, Y. (2023) Beyond knockouts: fine-tuning regulation of gene expression in plants with CRISPR-Cas-based promoter editing. *New Phytol.* **239**, 868–874.

Tang, X., Zheng, X., Qi, Y., Zhang, D., Cheng, Y., Tang, A., Voytas, D.F. *et al*. (2016) A single transcript CRISPR-Cas9 system for efficient genome editing in plants. *Mol. Plant*, **9**, 1088–1091.

Tang, X., Lowder, L.G., Zhang, T., Malzahn, A.A., Zheng, X., Voytas, D.F., Zhong, Z. *et al*. (2017) A CRISPR-Cpf1 system for efficient genome editing and transcriptional repression in plants. *Nat. Plants*, **3**, 17018.

Tang, X., Liu, G., Zhou, J., Ren, Q., You, Q., Tian, L., Xin, X. *et al*. (2018) A large-scale whole-genome sequencing analysis reveals highly specific genome editing by both Cas9 and Cpf1 (Cas12a) nucleases in rice. *Genome Biol.* **19**, 84.

Tang, X., Ren, Q., Yang, L., Bao, Y., Zhong, Z., He, Y., Liu, S. *et al*. (2019) Single transcript unit CRISPR 2.0 systems for robust Cas9 and Cas12a mediated plant genome editing. *Plant Biotechnol. J.* **17**, 1431–1445.

Tang, X., Sretenovic, S., Ren, Q., Jia, X., Li, M., Fan, T., Yin, D. *et al*. (2020) Plant prime editors enable precise gene editing in rice cells. *Mol. Plant*, **13**, 667–670.

Tang, X., Ren, Q., Yan, X., Zhang, R., Liu, L., Han, Q., Zheng, X. *et al*. (2024) Boosting genome editing in plants with single transcript unit surrogate reporter systems. *Plant Commun.* **5**, 100921.

Teng, F., Li, J., Cui, T., Xu, K., Guo, L., Gao, Q., Feng, G. *et al*. (2019) Enhanced mammalian genome editing by new Cas12a orthologs with optimized crRNA scaffolds. *Genome Biol.* **20**, 15.

Tian, Z., Qian, Q., Liu, Q., Yan, M., Liu, X., Yan, C., Liu, G. *et al*. (2009) Allelic diversities in rice starch biosynthesis lead to a diverse array of rice eating and cooking qualities. *Proc. Natl. Acad. Sci. USA*, **106**, 21760–21765.

Toki, S., Hara, N., Ono, K., Onodera, H., Tagiri, A., Oka, S. and Tanaka, H. (2006) Early infection of scutellum tissue with *Agrobacterium* allows high-speed transformation of rice. *Plant J.* **47**, 969–976.

Toth, E., Czene, B.C., Kulcsar, P.I., Krausz, S.L., Talas, A., Nyeste, A., Varga, E. *et al*. (2018) Mb- and FnCpf1 nucleases are active in mammalian cells: activities and PAM preferences of four wild-type Cpf1 nucleases and of their altered PAM specificity variants. *Nucleic Acids Res.* **46**, 10272–10285.

Toth, E., Varga, E., Kulcsar, P.I., Kocsis-Jutka, V., Krausz, S.L., Nyeste, A., Welker, Z. *et al*. (2020) Improved LbCas12a variants with altered PAM specificities further broaden the genome targeting range of Cas12a nucleases. *Nucleic Acids Res.* **48**, 3722–3733.

Van Eck, J., Keen, P. and Tjahjadi, M. (2019) *Agrobacterium tumefaciens*-Mediated transformation of tomato. *Methods Mol. Biol.* **1864**, 225–234.

Wang, Y., Cheng, X., Shan, Q., Zhang, Y., Liu, J., Gao, C. and Qiu, J.L. (2014) Simultaneous editing of three homoeoalleles in hexaploid bread wheat confers heritable resistance to powdery mildew. *Nat. Biotechnol.* **32**, 947–951.

Wang, M., Mao, Y., Lu, Y., Tao, X. and Zhu, J.K. (2017) Multiplex gene editing in rice using the CRISPR-Cpf1 system. *Mol. Plant*, **10**, 1011–1013.

Wang, J., Zhu, R., Meng, Q., Qin, H., Quan, R., Wei, P., Li, X. *et al*. (2024) A natural variation in OsDSK2a modulates plant growth and salt tolerance through phosphorylation by SnRK1A in rice. *Plant Biotechnol. J.* **22**, 1881–1896.

Wei, K.F. (2009) Establishment of high efficiency genetic transformation system of maize mediated by *Agrobacterium tumefaciens*. *Yi Chuan*, **31**, 1158–1170.

Wilusz, J.E., JnBaptiste, C.K., Lu, L.Y., Kuhn, C.D., Joshua-Tor, L. and Sharp, P.A. (2012) A triple helix stabilizes the 3′ ends of long noncoding RNAs that lack poly(A) tails. *Genes Dev.* **26**, 2392–2407.

Wu, Y., He, Y., Sretenovic, S., Liu, S., Cheng, Y., Han, Y., Liu, G. *et al*. (2022) CRISPR-BETS: a base-editing design tool for generating stop codons. *Plant Biotechnol. J.* **20**, 499–510.

Xie, X., Ma, X., Zhu, Q., Zeng, D., Li, G. and Liu, Y.G. (2017) CRISPR-GE: a convenient software toolkit for CRISPR-based genome editing. *Mol. Plant*, **10**, 1246–1249.

Xu, R., Qin, R., Li, H., Li, J., Yang, J. and Wei, P. (2019a) Enhanced genome editing in rice using single transcript unit CRISPR-LbCpf1 systems. *Plant Biotechnol. J.* **17**, 553–555.

Xu, Z., Xu, X., Gong, Q., Li, Z., Li, Y., Wang, S., Yang, Y. *et al*. (2019b) Engineering broad-spectrum bacterial blight resistance by simultaneously disrupting variable TALE-binding elements of multiple susceptibility genes in rice. *Mol. Plant*, **12**, 1434–1446.

You, Q., Zhong, Z., Ren, Q., Hassan, F., Zhang, Y. and Zhang, T. (2018) CRISPRMatch: an automatic calculation and visualization tool for high-throughput CRISPR genome-editing data analysis. *Int. J. Biol. Sci.* **14**, 858–862.

Yuste-Lisbona, F.J., Fernandez-Lozano, A., Pineda, B., Bretones, S., Ortiz-Atienza, A., Garcia-Sogo, B., Muller, N.A. *et al*. (2020) ENO regulates tomato fruit size through the floral meristem development network. *Proc. Natl. Acad. Sci. USA*, **117**, 8187–8195.

Zetsche, B., Gootenberg, J.S., Abudayyeh, O.O., Slaymaker, I.M., Makarova, K.S., Essletzbichler, P., Volz, S.E. *et al*. (2015) Cpf1 is a single RNA-guided endonuclease of a class 2 CRISPR-Cas system. *Cell*, **163**, 759–771.

Zetsche, B., Heidenreich, M., Mohanraju, P., Fedorova, I., Kneppers, J., DeGennaro, E.M., Winblad, N. *et al*. (2017) Multiplex gene editing by CRISPR-Cpf1 using a single crRNA array. *Nat. Biotechnol.* **35**, 31–34.

Zetsche, B., Abudayyeh, O.O., Gootenberg, J.S., Scott, D.A. and Zhang, F. (2020) A survey of genome editing activity for 16 Cas12a orthologs. *Keio J. Med.* **69**, 59–65.

Zhang, H., Li, Y. and Zhu, J.K. (2018) Developing naturally stress-resistant crops for a sustainable agriculture. *Nat. Plants*, **4**, 989–996.

Zhang, Z., Hua, L., Gupta, A., Tricoli, D., Edwards, K.J., Yang, B. and Li, W. (2019) Development of an *Agrobacterium*-delivered CRISPR/Cas9 system for wheat genome editing. *Plant Biotechnol. J.* **17**, 1623–1635.

Zhang, L., Zuris, J.A., Viswanathan, R., Edelstein, J.N., Turk, R., Thommandru, B., Rube, H.T. *et al*. (2021a) AsCas12a ultra nuclease facilitates the rapid generation of therapeutic cell medicines. *Nat. Commun.* **12**, 3908.

Zhang, Y., Ren, Q., Tang, X., Liu, S., Malzahn, A.A., Zhou, J., Wang, J. *et al*. (2021b) Expanding the scope of plant genome engineering with Cas12a orthologs and highly multiplexable editing systems. *Nat. Commun.* **12**, 1944.

Zhang, L., Li, G., Zhang, Y., Cheng, Y., Roberts, N., Glenn, S.E., DeZwaan-McCabe, D. *et al*. (2023) Boosting genome editing efficiency in human cells and plants with novel LbCas12a variants. *Genome Biol.* **24**, 102.

Zheng, X., Yang, L., Li, Q., Ji, L., Tang, A., Zang, L., Deng, K. *et al*. (2018) MIGS as a simple and efficient method for gene silencing in rice. *Front. Plant Sci.* **9**, 662.

Zheng, X., Zhang, S., Liang, Y., Zhang, R., Liu, L., Qin, P., Zhang, Z. *et al*. (2023) Loss-function mutants of OsCKX gene family based on CRISPR-Cas systems revealed their diversified roles in rice. *Plant Genome*, **16**, e20283.

Zhong, Z., Zhang, Y., You, Q., Tang, X., Ren, Q., Liu, S., Yang, L. *et al*. (2018) Plant genome editing using FnCpf1 and LbCpf1 nucleases at redefined and altered PAM sites. *Mol. Plant*, **11**, 999–1002.

Zhong, Z., Sretenovic, S., Ren, Q., Yang, L., Bao, Y., Qi, C., Yuan, M. *et al*. (2019) Improving plant genome editing with high-fidelity xCas9 and non-canonical PAM-targeting Cas9-NG. *Mol. Plant*, **12**, 1027–1036.

Zhong, Z., Liu, G., Tang, Z., Xiang, S., Yang, L., Huang, L., He, Y. *et al*. (2023) Efficient plant genome engineering using a probiotic sourced CRISPR-Cas9 system. *Nat. Commun.* **14**, 6102.

Zhou, J., Deng, K., Cheng, Y., Zhong, Z., Tian, L., Tang, X., Tang, A. *et al*. (2017) CRISPR-Cas9 based genome editing reveals new insights into MicroRNA function and regulation in rice. *Front. Plant Sci.* **8**, 1598.

Zhou, J., Xin, X., He, Y., Chen, H., Li, Q., Tang, X., Zhong, Z. *et al*. (2019) Multiplex QTL editing of grain-related genes improves yield in elite rice varieties. *Plant Cell Rep.* **38**, 475–485.

Zhou, J., Yuan, M., Zhao, Y., Quan, Q., Yu, D., Yang, H., Tang, X. *et al*. (2021) Efficient deletion of multiple circle RNA loci by CRISPR-Cas9 reveals Os06circ02797 as a putative sponge for OsMIR408 in rice. *Plant Biotechnol. J.* **19**, 1240–1252.

Zhou, J., Zhang, R., Jia, X., Tang, X., Guo, Y., Yang, H., Zheng, X. *et al*. (2022) CRISPR-Cas9 mediated OsMIR168a knockout reveals its pleiotropy in rice. *Plant Biotechnol. J.* **20**, 310–322.

Zhou, J., Liu, G., Zhao, Y., Zhang, R., Tang, X., Li, L., Jia, X. *et al*. (2023) An efficient CRISPR-Cas12a promoter editing system for crop improvement. *Nat. Plants*, **9**, 588–604.

Supporting information

Additional supporting information may be found online in the Supporting Information section at the end of the article.

Figure S1 Genotypes of T_0 plants edited by Mb3Cas12a at both TTTV and TTV PAM sites in rice. Protospacer and protospacer adjacent motif (PAM) were colour-coded in blue and red, respectively.

Figure S2 Analyses of genome editing profile in rice protoplasts. (a) Assessment of deletion frequencies by six Cas12a orthologs at the TTTG site in rice protoplasts at 32 °C. (b–d) Deletion size profile of Cas12a orthologs at TTTG site in rice protoplasts at 32 °C. (b) (HkCas12a), (c) (PrCas12a), (d) (Mb3Cas12a). (e–h) Assessment of protospacer length requirements at the *OsDEP1*-cR02 site in rice protoplasts. (f) (HkCas12a), (g) (PrCas12a), (h) (Mb3Cas12a). Three biological replicates were used. The error bars denote standard deviations.

Figure S3 Multiplexed editing by an Mb3Cas12a STU^{DD} system based on self-processing of the DR array. (a) The schematic diagram of the CRISPR-Mb3Cas12a STU^{DD} vector system based on the DR array self-processing. (b) Editing efficiency at three sites in rice T_0 lines. 15 independent T_0 lines were genotyped at each target site for wild type (denoted as an empty rectangle) and monoallelic mutant (denoted as a half-filled rectangle).

Figure S4 Genotypes of multiplex edited rice plants by two CRISPR-Mb3Cas12a systems. Genotypes of T_0 plants edited by Mb3Cas12a STU^{HDH} and Dual Pol II systems in rice. In both cases, dual ribozyme-based processing of crRNAs was used. PAM and spacer sequence were colour-coded in red and blue, respectively. The inserted sequence was colour-coded in purple.

Figure S5 Comparison of FnCas12a and HkCas12a coupled with DR and 4n96 DR-based editing efficiency at 4 target sites in rice protoplasts. The experiments in rice protoplasts were conducted at 32 °C, and three biological replicates were used. The error bars denote standard deviations.

Figure S6 Genome editing using Mb3Cas12a variants in rice protoplasts. (a) Sequence alignment showing the mutated amino acid in Mb3Cas12a-R, Mb3Cas12a-RRR, and Mb3Cas12a-RVRR compared to the wild-type Cas12a. (b) Schematics of Mb3Cas12a and its variants' vectors in the optimized STU^{HDH} expression system. (c, d) Editing profiles of Mb3Cas12a and its variants on one TTTV PAM site in rice protoplasts at 32 °C. (c) Mutation frequencies. Indel, insertions and deletions; (d) Deletion sizes. The mutation frequencies were calculated by amplicon sequencing. The error bars indicated the standard errors of three biological replicates.

Figure S7 Genotyping of promoter editing rice lines generated by the optimized CRISPR-Mb3Cas12a system. (a) Editing efficiency of Mb3Cas12a at the promoters of *OsGBSS1* and *OsD18* in rice T_0 lines. (b) Agarose gel electrophoresis analysis of mutations in the *OsGBSS1* promote target region in T_0 lines. The T_1 homozygous lines from #7, #9, #10 for the further study. (c) Agarose gel electrophoresis analysis of mutations in the *OsD18* promoter target region in T_0 lines. The T_1 homozygous lines from #11, #12, #13, #19 for the further study. ND, not detected.

Figure S8 Genotypes of five Mb3Cas12a-based *OsGBSS1* promoter (*OsGBSS1*-Pro) editing T_1 lines. PAM and spacer sequence were colour-coded in red and blue, respectively. The inserted sequence was colour-coded in purple.

Figure S9 Genotypes of four Mb3Cas12a-based *OsD18* promoter (*OsD18*-Pro) editing T_1 lines. PAM and spacer sequence were colour-coded in red and blue, respectively. The inserted sequence was colour-coded in purple.

Figure S10 Prediction of *ZmMIR159f* secondary structures in the maize mutants.

Figure S11 Cas12a coding sequences used in this study.

Figure S12 DNA sequences of Mb3Cas12a STU^{HDH} vectors with different linkers. (a–c) Vector's DNA sequences with different linkers ((a) PolyA; (b) Triplex; (c) Comp.14). SV40 NLS was colour-coded in red, Mb3Cas12a was in black, nucleoplasmin NLS was

colour-coded in dark blue, linker was highlighted with yellow ((a) PolyA; (b) Triplex; (c) Comp.14), HH was colour-coded in dark green, Mb3Cas12a DR was colour-coded in dark purple, crRNA was colour-coded in light blue, HDV was colour-coded in light green.

Figure S13 DNA sequences of Mb3Cas12a STU^{HDH} vectors with different NLS. (a–c) Vector's DNA sequences with different NLS ((a) NC NLS; (b) 3C NLS; (c) 2C NLS). SV40 NLS was highlighted with yellow, Mb3Cas12a was in black, nucleoplasmin NLS was highlighted with light purple, PolyA was colour-coded in red, HH was colour-coded in dark green, Mb3Cas12a DR was colour-coded in dark purple, crRNA was colour-coded in light blue, HDV was colour-coded in light green, HA tag was colour-coded in orange.

Table S1 Oligos used in this study.

Table S2 T-DNA constructs used in this study.

Table S3 crRNAs used in this study.